of SIRT1 has improved health and survival of mice on a high-calorie diet by ameliorating insulin resistance [9]. Here we demonstrated the expression of SIRT1 in human GCs by immunohistochemical and Western blot analysis, and the expression of its mRNA in rat GCs by RT-PCR. To our knowledge, this is the first report that SIRT1 is expressed in the ovarian follicular cells. It is also interesting that resveratrol treatment caused an increase in SIRT1 mRNA levels as well as the stimulation of the deacetylating function of SIRT1. Similar to this result, the mouse experimental model of dextran sodium sulfate-induced colitis was associated with a decrease in SIRT1 gene expression and resveratrol treatment significantly reversed the expression of SIRT1 [26]. However, it should be noted that all actions of resveratrol are not related to the activation of SIRT1 because resveratrol is an indirect activator of SIRT1 and has been shown to activate the expression and activity of nicotinamide phosphoribosyltransferase and AMP-activated protein kinase (AMPK) [27-30].

In our study, resveratrol increased the expression of P450arom and luteinization-related molecules, such as LH-R and StAR, in rat GCs, suggesting a possibility that resveratrol may promote steroidogenesis and luteinization, a process of terminal differentiation of GCs, in the ovary. In fact, P4 secretion was increased after resveratrol treatment. These findings are consistent with the previous study using HL60 promyelocytic cell line [31]. Since mRNA levels of LH-R in the human corpus luteum were reported to be about 7 times higher than those in preovulatory follicles [32], LH-R has been thought to be a key factor in the ability of GC to undergo luteinization. In the human and other primates, StAR is also essential for the development and maintenance of the corpus luteum. StAR is known to govern the rate-limiting step in steroidogenesis, which is the translocation of cholesterol from the outer to the inner mitochondrial membrane [33]. The process of luteinization is associated with up-regulation of StAR in luteinized granulosa cells. Considering the fact that StAR is not highly expressed in GCs of preovulatory follicles [34], our data may implicate a role of SIRT1 and its activator in promoting luteinization of the ovary. Following ovulation, GCs undergo luteinization and form the corpus luteum which secretes P4. Secretion of P4 is indispensable to cause secretory transformation of the endometrium so that implantation can occur. Before the placenta takes over P4 production, P4 produced by the corpus luteum provides the necessary support to early pregnancy. A defect in the corpus luteum function is associated with implantation failure and miscarriage [35]. Here we showed a new insight that the resveratrol treatment may serve, at least in part, as luteal support. Physiological roles of resveratrol in the ovary should be further determined because another possible beneficial effect on ovarian physiology is reported. Resveratrol is known as a pure aryl hydrocarbon receptor antagonist with no agonistic activity. Polycyclic aromatic hydrocarbons are environmental toxicants found in cigarette smoke, and stimulate aryl hydrocarbon receptor. Polycyclic aromatic hydrocarbons have detrimental effect on ovarian reserve via inducing Harakiri, and resveratrol may exert its rescuing effect by inhibiting Harakiri expression [36]. However, in view of the significant difference in the ovarian physiology between humans and rodents, our data should be interpreted with caution and the present observations should be verified using human GCs.

Conclusions

We have demonstrated that resveratrol plays a key role in the activation of luteinization, the terminal differentiation of GCs, and exerts its effects by stimulating the expression of SIRT1, StAR, LH-R, and P450arom in GCs. As a result of these effects, we found that resveratrol promoted P4 secretion. These results suggest that the stimulation of SIRT1 by resveratrol would be potentially beneficial in the treatment of luteal phase deficiency. Several chemical compounds are known to affect the SIRT1 activities, and SIRT1 stimulators are currently extensively investigated for the treatment of diabetes. We hypothesize that these drugs might have a role in ovarian physiology by affecting SIRT1, but further studies are necessary to confirm the physiological implication of SIRT1 in the ovary.

Abbreviations

DES: Diethylstilbestrol; DMEM: Dulbecco's Modified Eagle Medium; FBS: Fetal bovine serum; FSH-R: Follicle stimulating hormone receptor; GC: Granulosa cell; LH-R: Luteinizing hormone receptor; P4: Progesterone; P450arom: P450 aromatase; RT-PCR: Reverse transcript-polymerase chain reaction; StAR: Steroidogenic acute regulatory protein.

Acknowledgements

This study was supported by Grant-in-Aid for Scientific Research from the Ministry of Education, Science and Culture, JMS Bayer Schering Pharma Grant, Kowa Life Science Foundation, and Kanzawa Medical Research Foundation, Japan.

Author details

[1]Department of Obstetrics and Gynecology, Graduate School of Medicine, The University of Tokyo, 7-3-1, Hongo, Bunkyo-ku, Tokyo 113-8655, Japan. [2]Department of Obstetrics and Gynecology, School of Medicine, Teikyo University, 2-11-1 Kaga, Itabashi-ku, Tokyo 173-8605, Japan. [3]Laboratory of Integrative Brain Sciences, Department of Biology, Waseda University, 2-2, Wakamatsuchou, Shinjuku-ku, Tokyo, 162-8480, Japan.

Authors' contributions

YM carried out all of the experiments. AS, MH, HH, YM, and KS participated in the immunohistochemistry, real time PCR, Western blot, and hormonal quantification. OY helped to collect and purify rat GCs. SK, MH, and HO helped to collect human luteinized GCs from follicular aspirates. OW-H has been involved in acquisition of data, drafting the manuscript, and revising it critically for important intellectual content. KO, SN, and TY have made

substantial contributions to conception and design, analysis and interpretation of data. KT and YT have given final approval of the version to be submitted. All authors read and approved the final manuscript.

Competing interests
The authors declare that they have no competing interests.

Received: 5 September 2011 Accepted: 23 February 2012
Published: 23 February 2012

References

1. Langcake P, Pryce RJ: **A new class of phytoalexins from grapevines.** *Experientia* 1977, **33(2)**:151-152.
2. Gusman J, Malonne H, Atassi G: **A reappraisal of the potential chemopreventive and chemotherapeutic properties of resveratrol.** *Carcinogenesis* 2001, **22(8)**:1111-1117.
3. Jang M, Cai L, Udeani GO, Slowing KV, Thomas CF, Beecher CW, Fong HH, Farnsworth NR, Kinghorn AD, Mehta RG, *et al*: **Cancer chemopreventive activity of resveratrol, a natural product derived from grapes.** *Science* 1997, **275(5297)**:218-220.
4. Manna SK, Mukhopadhyay A, Aggarwal BB: **Resveratrol suppresses TNF-induced activation of nuclear transcription factors NF-kappa B, activator protein-1, and apoptosis: potential role of reactive oxygen intermediates and lipid peroxidation.** *J Immunol* 2000, **164(12)**:6509-6519.
5. Joe AK, Liu H, Suzui M, Vural ME, Xiao D, Weinstein IB: **Resveratrol induces growth inhibition, S-phase arrest, apoptosis, and changes in biomarker expression in several human cancer cell lines.** *Clin Cancer Res* 2002, **8(3)**:893-903.
6. van Ginkel PR, Sareen D, Subramanian L, Walker Q, Darjatmoko SR, Lindstrom MJ, Kulkarni A, Albert DM, Polans AS: **Resveratrol inhibits tumor growth of human neuroblastoma and mediates apoptosis by directly targeting mitochondria.** *Clin Cancer Res* 2007, **13(17)**:5162-5169.
7. Issuree PD, Pushparaj PN, Pervaiz S, Melendez AJ: **Resveratrol attenuates C5a-induced inflammatory responses in vitro and in vivo by inhibiting phospholipase D and sphingosine kinase activities.** *FASEB J* 2009, **23(8)**:2412-2424.
8. Howitz KT, Bitterman KJ, Cohen HY, Lamming DW, Lavu S, Wood JG, Zipkin RE, Chung P, Kisielewski A, Zhang LL, *et al*: **Small molecule activators of sirtuins extend Saccharomyces cerevisiae lifespan.** *Nature* 2003, **425(6954)**:191-196.
9. Baur JA, Pearson KJ, Price NL, Jamieson HA, Lerin C, Kalra A, Prabhu VV, Allard JS, Lopez-Lluch G, Lewis K, *et al*: **Resveratrol improves health and survival of mice on a high-calorie diet.** *Nature* 2006, **444(7117)**:337-342.
10. Michan S, Sinclair D: **Sirtuins in mammals: insights into their biological function.** *Biochem J* 2007, **404(1)**:1-13.
11. Finkel T, Deng CX, Mostoslavsky R: **Recent progress in the biology and physiology of sirtuins.** *Nature* 2009, **460(7255)**:587-591.
12. Wong DH, Villanueva JA, Cress AB, Duleba AJ: **Effects of resveratrol on proliferation and apoptosis in rat ovarian theca-interstitial cells.** *Mol Hum Reprod* 2010, **16(4)**:251-259.
13. Basini G, Tringali C, Baioni L, Bussolati S, Spatafora C, Grasselli F: **Biological effects on granulosa cells of hydroxylated and methylated resveratrol analogues.** *Mol Nutr Food Res* 2010, **54(Suppl 2)**:S236-243.
14. Nishi Y, Yanase T, Mu Y, Oba K, Ichino I, Saito M, Nomura M, Mukasa C, Okabe T, Goto K, *et al*: **Establishment and characterization of a steroidogenic human granulosa-like tumor cell line, KGN, that expresses functional follicle-stimulating hormone receptor.** *Endocrinology* 2001, **142(1)**:437-445.
15. Shi J, Yoshino O, Osuga Y, Nishii O, Yano T, Taketani Y: **Bone morphogenetic protein 7 (BMP-7) increases the expression of follicle-stimulating hormone (FSH) receptor in human granulosa cells.** *Fertil Steril* 2010, **93(4)**:1273-1279.
16. Otsuka F, Moore RK, Wang X, Sharma S, Miyoshi T, Shimasaki S: **Essential role of the oocyte in estrogen amplification of follicle-stimulating hormone signaling in granulosa cells.** *Endocrinology* 2005, **146(8)**:3362-3367.
17. Chen Q, Yano T, Matsumi H, Osuga Y, Yano N, Xu J, Wada O, Koga K, Fujiwara T, Kugu K, *et al*: **Cross-Talk between Fas/Fas ligand system and nitric oxide in the pathway subserving granulosa cell apoptosis: a possible regulatory mechanism for ovarian follicle atresia.** *Endocrinology* 2005, **146(2)**:808-815.
18. Wada-Hiraike O, Hiraike H, Okinaga H, Imamov O, Barros RP, Morani A, Omoto Y, Warner M, Gustafsson JA: **Role of estrogen receptor beta in uterine stroma and epithelium: Insights from estrogen receptor beta-/- mice.** *Proc Natl Acad Sci USA* 2006, **103(48)**:18350-18355.
19. Hiraike H, Wada-Hiraike O, Nakagawa S, Koyama S, Miyamoto Y, Sone K, Tanikawa M, Tsuruga T, Nagasaka K, Matsumoto Y, *et al*: **Identification of DBC1 as a transcriptional repressor for BRCA1.** *Br J Cancer* 2010, **102(6)**:1061-1067.
20. Kim JE, Lou Z, Chen J: **Interactions between DBC1 and SIRT 1 are deregulated in breast cancer cells.** *Cell Cycle* 2009, **8(22)**:3784-3785.
21. Kim JE, Chen J, Lou Z: **DBC1 is a negative regulator of SIRT1.** *Nature* 2008, **451(7178)**:583-586.
22. Zhao W, Kruse JP, Tang Y, Jung SY, Qin J, Gu W: **Negative regulation of the deacetylase SIRT1 by DBC1.** *Nature* 2008, **451(7178)**:587-590.
23. Henry LA, Witt DM: **Resveratrol: phytoestrogen effects on reproductive physiology and behavior in female rats.** *Horm Behav* 2002, **41(2)**:220-228.
24. Bowers JL, Tyulmenkov VV, Jernigan SC, Klinge CM: **Resveratrol acts as a mixed agonist/antagonist for estrogen receptors alpha and beta.** *Endocrinology* 2000, **141(10)**:3657-3667.
25. Gehm BD, McAndrews JM, Chien PY, Jameson JL: **Resveratrol, a polyphenolic compound found in grapes and wine, is an agonist for the estrogen receptor.** *Proc Natl Acad Sci USA* 1997, **94(25)**:14138-14143.
26. Singh UP, Singh NP, Singh B, Hofseth LJ, Price RL, Nagarkatti M, Nagarkatti PS: **Resveratrol (trans-3,5,4'-trihydroxystilbene) induces silent mating type information regulation-1 and down-regulates nuclear transcription factor-kappaB activation to abrogate dextran sulfate sodium-induced colitis.** *J Pharmacol Exp Ther* 2010, **332(3)**:829-839.
27. Hou X, Xu S, Maitland-Toolan KA, Sato K, Jiang B, Ido Y, Lan F, Walsh K, Wierzbicki M, Verbeuren TJ, *et al*: **SIRT1 regulates hepatocyte lipid metabolism through activating AMP-activated protein kinase.** *J Biol Chem* 2008, **283(29)**:20015-20026.
28. Suchankova G, Nelson LE, Gerhart-Hines Z, Kelly M, Gauthier MS, Saha AK, Ido Y, Puigserver P, Ruderman NB: **Concurrent regulation of AMP-activated protein kinase and SIRT1 in mammalian cells.** *Biochem Biophys Res Commun* 2009, **378(4)**:836-841.
29. Um JH, Park SJ, Kang H, Yang S, Foretz M, McBurney MW, Kim MK, Viollet B, Chung JH: **AMP-activated protein kinase-deficient mice are resistant to the metabolic effects of resveratrol.** *Diabetes* 2010, **59(3)**:554-563.
30. Chung S, Yao H, Caito S, Hwang JW, Arunachalam G, Rahman I: **Regulation of SIRT1 in cellular functions: role of polyphenols.** *Arch Biochem Biophys* 2010, **501(1)**:79-90.
31. Ragione FD, Cucciolla V, Borriello A, Pietra VD, Racioppi L, Soldati G, Manna C, Galletti P, Zappia V: **Resveratrol arrests the cell division cycle at S/G2 phase transition.** *Biochem Biophys Res Commun* 1998, **250(1)**:53-58.
32. Minegishi T, Tano M, Abe Y, Nakamura K, Ibuki Y, Miyamoto K: **Expression of luteinizing hormone/human chorionic gonadotrophin (LH/HCG) receptor mRNA in the human ovary.** *Mol Hum Reprod* 1997, **3(2)**:101-107.
33. Devoto L, Kohen P, Vega M, Castro O, Gonzalez RR, Retamales I, Carvallo P, Christenson LK, Strauss JF: **Control of human luteal steroidogenesis.** *Mol Cell Endocrinol* 2002, **186(2)**:137-141.
34. Kiriakidou M, McAllister JM, Sugawara T, Strauss JF: **Expression of steroidogenic acute regulatory protein (StAR) in the human ovary.** *J Clin Endocrinol Metab* 1996, **81(11)**:4122-4128.
35. Devoto L, Kohen P, Munoz A, Strauss JF: **Human corpus luteum physiology and the luteal-phase dysfunction associated with ovarian stimulation.** *Reprod Biomed Online* 2009, **18(Suppl 2)**:19-24.
36. Jurisicova A, Taniuchi A, Li H, Shang Y, Antenos M, Detmar J, Xu J, Matikainen T, Benito Hernandez A, Nunez G, *et al*: **Maternal exposure to polycyclic aromatic hydrocarbons diminishes murine ovarian reserve via induction of Harakiri.** *J Clin Invest* 2007, **117(12)**:3971-3978.

doi:10.1186/1477-7827-10-14
Cite this article as: Morita *et al.*: Resveratrol promotes expression of SIRT1 and StAR in rat ovarian granulosa cells: an implicative role of SIRT1 in the ovary. *Reproductive Biology and Endocrinology* 2012 10:14.

British Journal of Cancer (2011) 104, 1349 – 1355

www.bjcancer.com

Multifunctional transcription factor TFII-I is an activator of BRCA1 function

M Tanikawa[1], O Wada-Hiraike*[,1], S Nakagawa[1], A Shirane[1], H Hiraike[1], S Koyama[1], Y Miyamoto[1], K Sone[1], T Tsuruga[1], K Nagasaka[1], Y Matsumoto[1], Y Ikeda[1], K Shoji[1], K Oda[1], H Fukuhara[2], K Nakagawa[3], S Kato[4], T Yano[1] and Y Taketani[1]

[1]Department of Obstetrics and Gynecology, Graduate School of Medicine, The University of Tokyo, 7-3-1 Hongo, Bunkyo-ku, Tokyo 113-8655, Japan; [2]Department of Urology, Graduate School of Medicine, The University of Tokyo, 7-3-1 Hongo, Bunkyo-ku, Tokyo 113-8655, Japan; [3]Department of Radiology, Graduate School of Medicine, The University of Tokyo, 7-3-1 Hongo, Bunkyo-ku, Tokyo 113-8655, Japan; [4]Institute of Molecular and Cellular Biosciences, The University of Tokyo, 1-1-1 Yayoi, Bunkyo-ku, Tokyo 113-0034, Japan

BACKGROUND: The TFII-I is a multifunctional transcriptional factor known to bind specifically to several DNA sequence elements and to mediate growth factor signalling. A microdeletion at the chromosomal location 7q11.23 encoding TFII-I and the related family of transcription factors may result in the onset of Williams–Beuren syndrome, an autosomal dominant genetic disorder characterised by a unique cognitive profile, diabetes, hypertension, anxiety, and craniofacial defects. Hereditary breast and ovarian cancer susceptibility gene product BRCA1 has been shown to serve as a positive regulator of SIRT1 expression by binding to the promoter region of SIRT1, but cross talk between BRCA1 and TFII-I has not been investigated to date.

METHODS: A physical interaction between TFII-I and BRCA1 was explored. To determine pathophysiological function of TFII-I, its role as a transcriptional cofactor for BRCA1 was investigated.

RESULTS: We found a physical interaction between the carboxyl terminus of TFII-I and the carboxyl terminus of BRCA1, also known as the BRCT domain. Endogenous TFII-I and BRCA1 form a complex in nuclei of intact cells and formation of irradiation-induced nuclear foci was observed. We also showed that the expression of TFII-I stimulates the transcriptional activation function of BRCT by a transient expression assay. The expression of TFII-I also enhanced the transcriptional activation of the SIRT1 promoter mediated by full-length BRCA1.

CONCLUSION: These results revealed the intrinsic mechanism that TFII-I may modulate the cellular functions of BRCA1, and provide important implications to understand the development of breast cancer.

British Journal of Cancer (2011) **104,** 1349–1355. doi:10.1038/bjc.2011.75 www.bjcancer.com
Published online 15 March 2011

Keywords: TFII-I; BRCA1; interaction; activation; DNA damage repair

The TFII-I was identified originally as a factor that could bind to two distinct promoter elements, the pyrimidine-rich initiator and the recognition site (E-box) for upstream factor 1. The TFII-I stimulates transcription from the potent TATA- and initiator-containing adenovirus major late promoter (AdMLP) synergistically with upstream factor 1 (Roy *et al*, 1997). The TFII-I is a unique multifunctional factor that selectively regulates gene expressions when activated by a variety of extracellular signals and can function both as a basal transcriptional factor and as an activator (Roy, 2007). An autosomal dominant genetic disorder Williams–Beuren syndrome is a multisystem disorder characterised by distinctive facial features, mental disability, diabetes mellitus, and supravalvular aortic stenosis. The haploinsufficiency for TFII-I is causative to the craniofacial phenotype in humans (Pober, 2010). The primary structure of TFII-I is compatible with its multifunctional properties, consisting of six direct reiterated I-repeats, R1–R6, each containing a putative helix-loop-helix motif (Roy, 2007). The I-repeats are postulated to be protein interaction surfaces. Given those multifunctional features and structural characteristics, it is important to investigate the role of the I-repeats in mediating protein interactions and to search for proteins that make complex with TFII-I through this domain.

The breast cancer susceptibility gene *BRCA1* encodes a phosphoprotein that is involved in ubiquitination, DNA damage response, regulation of cell cycle checkpoints, and transcriptional regulation. Binding to the transcriptional machinery by the carboxyl terminal BRCA1, referred to as BRCT domain, was the first biochemical activity ascribed to the BRCA1 protein (Anderson *et al*, 1998). In addition, BRCT has been shown to be involved in double-stranded DNA repair and homologous recombination (Callebaut and Mornon, 1997; Moynahan *et al*, 1999; Zhong *et al*, 1999). On the basis of the data that targeted deletion of the BRCT domain results in embryonic lethality (Hohenstein *et al*, 2001), BRCT is postulated to be indispensable for the normal cellular growth, and it would be intriguing to investigate physiological functions of BRCT. BRCA1 carboxyl-terminal domain (BRCT) possesses the autonomous transcriptional activation

*Correspondence: Dr O Wada-Hiraike; E-mail: osamu.hiraike@gmail.com
Received 22 October 2010; revised 31 January 2011; accepted 8 February 2011; published online 15 March 2011

function when the BRCT domain is fused to a GAL4 DNA-binding domain (Monteiro *et al*, 1996). The point mutations in the BRCT domain derived from patients with inherited breast cancer result in loss of transcriptional activity (Chapman and Verma, 1996). The BRCT domain has been shown to be an interaction surface with a number of transcription factors and co-regulators (Saka *et al*, 1997; Wada *et al*, 2004; Oishi *et al*, 2006; Hiraike *et al*, 2010).

To better understand the functional significance and the transcriptional regulation of BRCT, we previously have searched for putative transcription coactivator complexes that interact with the BRCT domain using a biochemical approach (Wada *et al*, 2004; Oishi *et al*, 2006). During these studies, we preliminary found that TFII-I interacted with the BRCT domain. Here, we confirmed that the carboxyl terminus of TFII-I and BRCA1 form a complex *in vivo*. We further studied the effect on transcriptional regulation of BRCA1 driven by TFII-I. These findings establish a principal biological function of TFII-I as an activator of BRCA1 function, and identify TFII-I as a possible determinant of breast cancer.

MATERIALS AND METHODS

Cell culture

Human cervical adenocarcinoma HeLa (CCL-2), HCC1937 (CRL-2336) breast cancer cells that express a carboxyl-terminally truncated BRCA1 protein (Scully *et al*, 1999), and African green monkey kidney fibroblast-like COS7 (CRL-1651) cell lines were purchased from the American Type Culture Collection (Manassas, VA, USA). HeLa and COS7 cells were maintained in Dulbecco's modified Eagle medium supplemented with 10% fetal bovine serum. HCC1937 cells were maintained in RPMI medium supplemented with 10% fetal bovine serum.

Plasmid construction

BRCA1 expression vectors, BRCT vectors and reporter constructs (17M8-AdMLP-luc and SIRT1-luc) were described previously (Wada *et al*, 2004; Hiraike *et al*, 2010). TFII-I expression vectors were described previously (Cheriyath and Roy, 2001).

Chemicals and antibodies

Rabbit antibodies were anti-TFII-I, anti-BRCA1, and anti-GST (Cell Signaling Technology Inc., Temecula, CA, USA, catalogue no. #4562, #9010, and #2622, respectively). Mouse monoclonal antibodies were anti-BRCA1 (Calbiochem, EMD Biosciences Inc., La Jolla, CA, USA, catalogue no. OP107), anti-SIRT1 (Abcam Ltd., Cambridge, UK, catalogue no. ab32441), and HRP-conjugated anti-Flag (Abcam Ltd., catalogue no. ab49763). Anti-BRCA1 (catalogue no. sc-642), anti-p53 (catalogue no. sc-126), and anti-Actin (catalogue no. sc-47778) were purchased from Santa Cruz Biotechnology Inc. (Santa Cruz, CA, USA). Alexa Fluor 488 conjugated donkey anti-mouse IgG (catalogue no. A-21202) and Alexa Fluor 568 conjugated goat anti-rabbit IgG (catalogue no. A-11011) were purchased from Invitrogen (Carlsbad, CA, USA).

Immunoprecipitation and western blot

The formation of a TFII-I-BRCA1 complex in HeLa, HCC1937, and COS7 cells was analysed by immunoprecipitation. The whole-cell extracts of HeLa and HCC1937 cells were applied for immunoprecipitation with anti-BRCA1 antibodies or preimmune IgG. The immunoprecipitates were subjected to 30 μl of protein G sepharose 4 Fast Flow (GE healthcare UK Ltd., Buckinghamshire, UK) and subsequently immunoblotted by anti-TFII-I antibodies. Reciprocal immunoprecipitation was also performed. COS7 cells transfected with indicated plasmids were lysed, fractionated, and subjected to anti-FLAG M2 agarose (Sigma-Aldrich, St Louis, MO, USA). Immunoprecipitated materials were blotted with anti-GST antibodies to identify TFII-I-containing complexes.

RNAi

The ablation of TFII-I and BRCA1 was performed by transfection of HeLa cells with siRNA duplex oligos synthesised by Qiagen (Hilden, Germany). Cells were transfected with control siRNA (AllStars Negative Control siRNA, 1027281), TFII-I-specific siRNA (TFII-I-RNAi: 5′-AAACGGAGCCUACUGAACA-3′, which covered mRNA regions of nucleotides 956–974 (amino acids 195–201) of TFII-I), DBC1-specific siRNA (DBC1-RNAi: 5′-AAACGGAGCCUA CUGAACA-3′, which covered mRNA regions of nucleotides 1379–1397 (amino acids 460–466) of DBC1), and BRCA1-specific siRNA (SI02664361) using HiperFect reagent (Qiagen).

GST-pull down assay

Glutathione-S-transferase fusion proteins or GST alone were expressed in *Escherichia coli* and immobilised on glutathione-sepharose 4B beads (GE healthcare UK Ltd.). The GST proteins were incubated with nuclear extracts of HeLa cells. Unbound proteins were removed and specifically bound proteins were eluted and analysed by SDS–PAGE.

Luciferase assay

Transfection was performed with Effectene reagent (Qiagen) or Lipofectamine 2000 (Invitrogen) according to the manufacturer's recommendation. For luciferase assay, cells were transfected with indicated expression vectors and/or GAL4 vectors. Reporter plasmids (17M8-AdMLP-luc or SIRT1-luc) were also cotransfected. As an internal control to equalise transfection efficiency, phRL CMV-*Renilla* vector (Promega Co., Madison, WI, USA) was also transfected in all the experiments. Individual transfections, each consisting of triplicate wells, were repeated at least three times as described previously (Wada *et al*, 2004).

Fluorescence microscopy

HeLa cells were grown on 12 mm BD BioCoat glass coverslips (BD Biosciences, San Jose, CA, USA, 354085) in 6-well plates. The cells were exposed to 8-gray (Gy) of γ-irradiation, fixed with PBS containing 4% paraformaldehyde and permeabilised in PBS with 0.2% (v/v) Triton X-100. After blocking, the cells were incubated sequentially with anti-BRCA1 and anti-TFII-I antibodies. Secondary antibodies were Alexa Fluor 488 conjugated donkey anti-mouse IgG, or Alexa Fluor 568 conjugated goat anti-rabbit IgG. The slides were briefly counter-stained and analysed under the confocal fluorescence microscope (Carl-Zeiss MicroImaging Inc., Oberkochen, Germany). Quantification of colocalisation was analysed using LSM7 series-ZEN200x software (Carl-Zeiss Micro-Imaging Inc.), and the ratio of colocalisation pixels *vs* total pixels in the target area was measured.

Chromatin immunoprecipitation assay

Preparation of soluble HeLa chromatin for PCR amplification was performed essentially as described (Oishi *et al*, 2006; Hiraike *et al*, 2010). Subconfluent HeLa cells were cross-linked with 1.5% formaldehyde at room temperature for 15 min, and washed twice with ice-cold PBS. The cell pellet was then resuspended in 0.2 ml lysis buffer and sonicated by Bioruptor UCD-250 (Cosmo Bio Co. Ltd., Tokyo, Japan). The sheared soluble chromatin was then subjected to immunoprecipitation with specific antibodies and protein G-sepharose equilibrated with salmon sperm DNA (Millipore, Upstate, Billerica, MA, USA). After extensive wash,

the beads were eluted. The eluate was incubated for 6 h at 65°C to reverse the formaldehyde cross-linking. The extracted DNA was purified with the use of QIAquick PCR purification kit (Qiagen). Polymerase chain reaction was performed using specific primers for the SIRT1 promoter (Wang *et al*, 2008; Hiraike *et al*, 2010) and the p21 promoter (Oishi *et al*, 2006).

RESULTS

TFII-I and BRCA1 interact *in vivo*

The pull-down products of nuclear extracts from HeLa cells through GST-BRCT column were separated by SDS-PAGE. In consistent with our preliminary result, we confirmed that TFII-I proteins interact with GST-BRCT by western blot (Figure 1A). To determine the interaction between the endogenous TFII-I and BRCA1 in cultured human cells, whole-cell lysates of HeLa cells were immunoprecipitated with anti-BRCA1 antibodies (epitope mapping at the carboxyl-terminus of BRCA1). The immunoblotting analysis using anti-TFII-I antibodies revealed the existence of TFII-I in cell lysate immunoprecipitates (Figure 1B, 1), which indicates that TFII-I physically associates with BRCA1 in living cells. The whole-cell extracts of HCC1937 cells known to lack last BRCT domain were also immunoprecipitated with anti-BRCA1 antibodies (epitope mapping at the amino-terminus of BRCA1). The immunoblotting analysis revealed the absence of TFII-I in cell lysate immunoprecipitates, which reinforced the importance of BRCT domain as the interaction surface with TFII-I (Figure 1B, 2). These data indicated that TFII-I interacted with BRCA1 through the BRCT domain. Reciprocal immunoprecipitation analysis confirmed this association (Figure 1B, 3).

To identify the regions of TFII-I that are responsible for the interaction with BRCT, deletion mutants of TFII-I were used for the assay. COS7 cells were transfected with Flag-tagged BRCA1 and GST-tagged TFII-I and nuclear extracts of transfected cells were immunoprecipitated with the anti-FLAG M2 agarose beads. Western blotting analysis with anti-GST antibodies revealed the existence of GST-tagged TFII-I in the protein extract of immunoprecipitates (Figure 1C), confirming that BRCA1 forms a complex with TFII-I. Flag-tagged BRCA1 and deletion mutants of GST-tagged TFII-I were also subjected to immunoprecipitation. TFII-I lacking the amino terminal region (TFII-I ΔN90) also interacted with BRCA1, while TFII-I lacking carboxyl terminus (TFII-I p70 and p46) showed no interaction with BRCA1. Immunoprecipitation using cytoplasmic fraction of the COS7 cells was also performed and TFII-I was not co-immunoprecipitated with BRCA1. These findings indicate that the carboxyl terminus (R3-R6) of TFII-I and the BRCT domain are both necessary and sufficient for the interaction between TFII-I and BRCA1 in cultured cells.

TFII-I and BRCA1 form endogenous complex in intact cells and nuclear foci in DNA-damaged cells

As BRCA1 and TFII-I interact *in vivo*, it was of interest to examine the subcellular distribution of these two proteins. To this end, immunofluorescence analysis was performed on HeLa cells. More than 80% substantial colocalisation signal (Merge) of BRCA1 (Alexa Fluor 488-conjugated anti-mouse IgG, green) and TFII-I (Alexa Fluor 568-conjugated anti-rabbit IgG, red) was observed in nuclei in control cells. Therefore, protein complexes containing both BRCA1 and TFII-I are likely to be distributed throughout nuclei. This result also implied the importance of nuclear localisation signal for the colocalisation of BRCA1 and TFII-I in nuclei. The previous study demonstrated that BRCA1 has been shown to display discrete nuclear foci after treatment of cells with irradiation (Zhong *et al*, 1999). HeLa cells irradiated with 8-Gy γ radiation demonstrated the punctate pattern of immunostaining

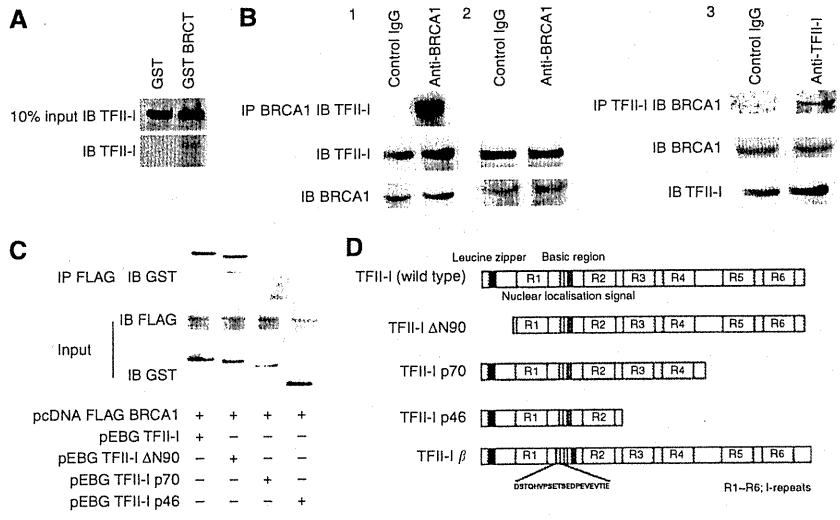

Figure 1 *In vivo* and *in vitro* association between TFII-I and BRCA1, and mapping of the BRCT-interacting region of TFII-I. (**A**) Identification of the interaction between BRCT and TFII-I using GST-BRCT. Bacterially expressed GST fusion proteins immobilised on beads were used in *in vitro* pull-down assays. Nuclear extracts of HeLa cells were incubated with GST-BRCT. The beads were extensively washed, and followed by immunoblotting (IB) using anti-TFII-I antibodies. (**B**) The complex formation of TFII-I and BRCA1 in HeLa cells was analysed by co-immunoprecipitation (IP) with the antibodies to BRCA1 (epitope mapping at the carboxyl-terminus of BRCA1). The immunoblotting analysis using anti-TFII-I antibodies revealed the existence of TFII-I in cell lysate immunoprecipitates (Figure 1B, 1), which indicates that TFII-I physically associates with BRCA1 in living cells. Reciprocal immunoprecipitation analysis confirmed the association of TFII-I and BRCA1 (Figure 1B, 3). The whole-cell extracts of HCC1937 cells known to lack last BRCT domain were also immunoprecipitated with anti-BRCA1 antibodies (epitope mapping at the amino-terminus of BRCA1). The immunoblotting analysis revealed the absence of TFII-I in cell lysate immunoprecipitates (Figure 1B, 2), indicating the importance of BRCT as a binding surface of TFII-I. (**C**) Mapping of the BRCT-interaction region of TFII-I. COS7 cells were transfected with GST-tagged TFII-I (wild type, ΔN90, p70, and p46) and Flag-tagged BRCA1 expression vectors. Nuclear extracts of transfected COS7 cells were prepared and the complex formation of TFII-I and BRCA1 was analysed by IP with the anti-Flag M2 agarose beads, followed by IB using anti-GST antibodies. (**D**) A schematic diagram of the structure of TFII-I (wild type, ΔN90, p70, p46, and β isoform) is shown.

for BRCA1 and this pattern overlap TFII-I-containing foci in HeLa cells (Figure 2B, 1–3). These data indicated that double strand DNA damage lead to the nuclear accumulation of the BRCA1-TFII-I complex, possibly at the site of double strand DNA-damage.

TFII-I enhances the transcriptional activation of BRCT

The result that the BRCT domain interacts with TFII-I led us to examine role of TFII-I in the transactivation function of GAL4-fused BRCT. Transient transfection assays were performed using a 17M8-AdMLP-luc luciferase reporter plasmid, carrying eight tandem repeat GAL4 DNA-binding sites (17M × 8) upstream of AdMLP driving expression of the firefly luciferase gene. The TFII-I alone had no effect on this luciferase reporter construct (Figure 3, lanes 2–6). Although GAL4-BRCT fusion protein (GAL-BRCT) activated the promoter activity of the reporter plasmid in COS7 cells, the transcriptional activity of BRCT was significantly stimulated by the expression of TFII-I at best two-fold on the artificial promoter in luciferase assays (Figure 3, lanes 7–8). Although TFII-I ΔN90 possessing the BRCT binding domain stimulated the transcriptional activation of GAL-BRCT, TFII-I lacking an interaction domain with BRCA1 (TFII-I p70 and p46) lost its ability to stimulate the BRCT-mediated transcriptional activation (Figure 3, lanes 9–11). The mammalian TFII-I has four spliced isoforms: α, β, γ, and Δ (wild type). Upon serum starvation, the β and Δ isoforms exhibits subcellular distribution changes in murine NIH3T3 cells (Hakre *et al*, 2006). The experimental data showed that TFII-I β also stimulated the transcriptional activation of BRCT (Figure 3, lane 12). These results suggest that carboxyl terminus of TFII-I has a significant role in the stimulation of BRCT-dependent transactivation.

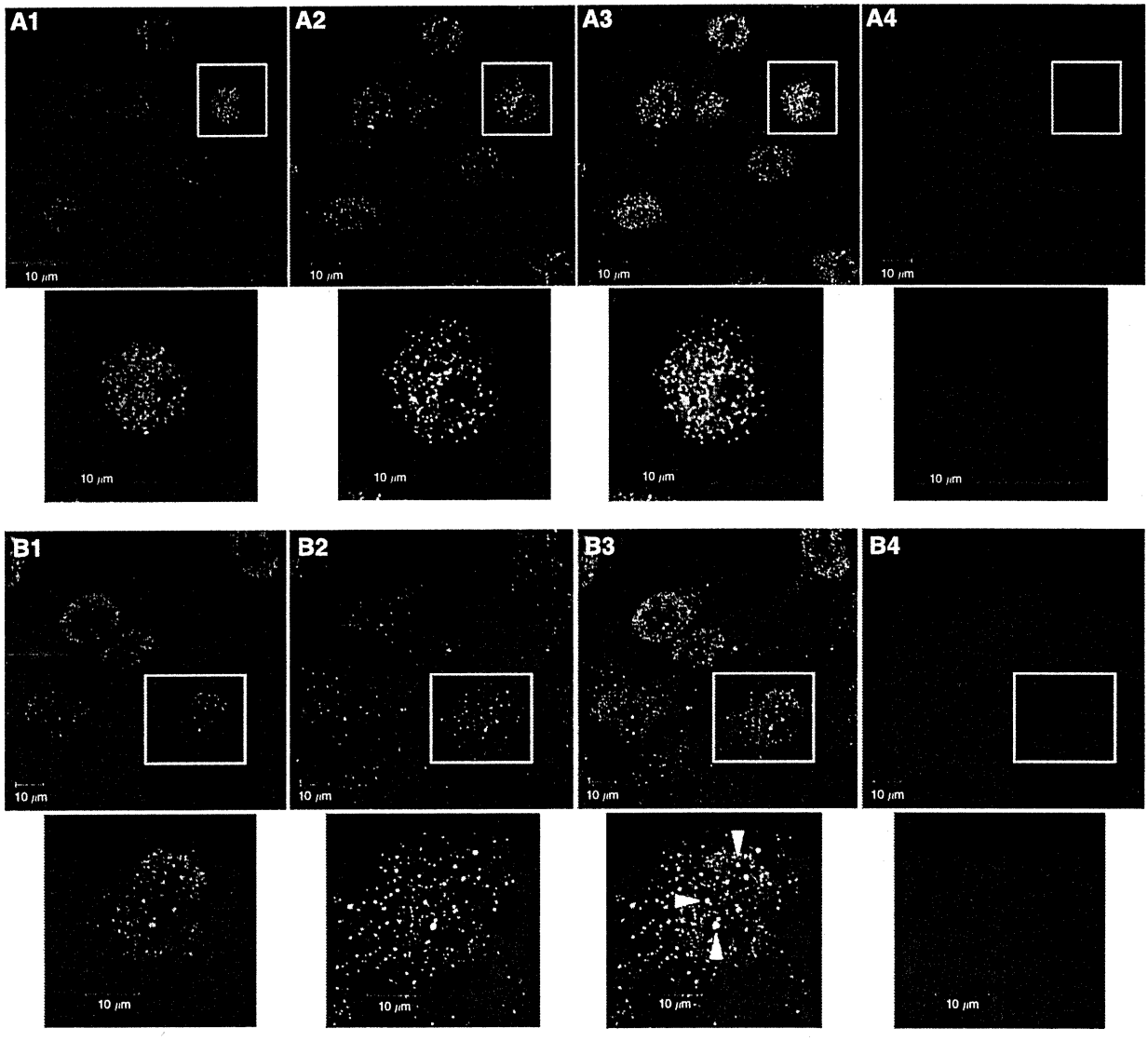

Figure 2 Colocalisation of BRCA1 and TFII-I in HeLa cells. (**A**–**D**) HeLa cells were either treated by 8-Gy of gamma-irradiation or none, fixed, and permeabilised. The cells were incubated with primary antibodies and subsequently with secondary antibodies. The expression of BRCA1 (green) and TFII-I (red) was investigated under the confocal fluorescence microscopy (Carl-Zeiss). Representative immunofluorescence studies are shown (**A**, control cells; **B**, irradiated cells; 1, TFII-I; 2, BRCA1; 3, merge; 4, 4′, 6-diamino-2-phenylindole staining). Arrows in B3 indicate a cell showing nuclear foci formation of TFII-I and BRCA1. Bars indicate 10 μm.

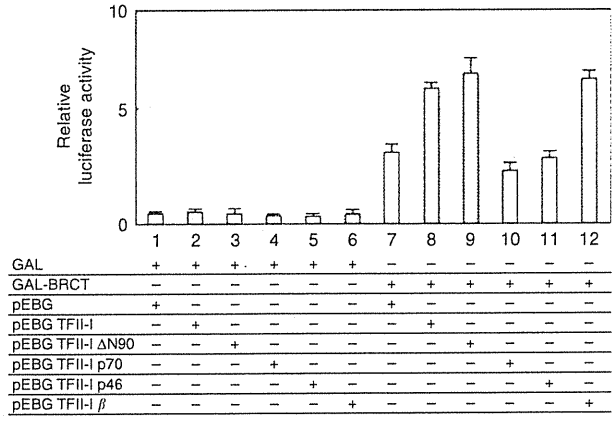

Figure 3 TFII-I stimulates transcription of GAL4-BRCT through its carboxyl-terminal domain. Transient transfection assays were performed to examine the cofactor activity of TFII-I in the transactivation function of GAL4-fused BRCT. COS7 cells were transfected with the indicated combinations of mammalian expression plasmids. At 24 h after transfection, the cells were harvested, and transfected whole-cell lysates were assayed for luciferase activity produced from the reporter plasmid (17M8-AdMLP-luc). TFII-I showed a specific stimulation of the transactivation function of BRCT. Carboxyl-terminus of TFII-I was indispensable for this stimulation of BRCT. The phRL *Renilla* CMV-luc vector was transfected as a control of transfection efficiency. Each experiment was repeated at least three times in triplicate. Error bars represent s.d.

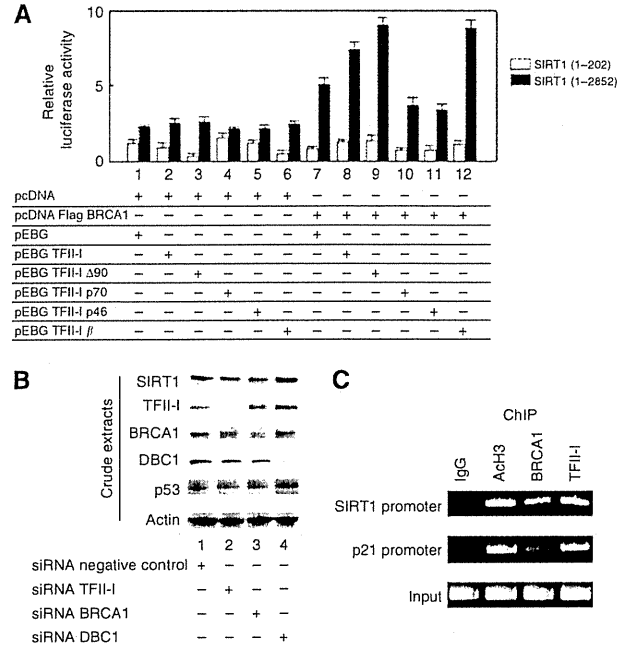

Figure 4 TFII-I stimulates transcription by BRCA1 through its carboxyl-terminal domain. (**A**) Transient transfection assays were performed to examine the influence of TFII-I using an artificial luciferase reporter constructs. COS7 cells were transfected with the indicated combinations of mammalian expression plasmids. At 24 h after transfection, cells were harvested, and transfected whole-cell lysates were assayed for luciferase activity produced from the reporter plasmids. Full-length TFII-I and TFII-I ΔN90 showed specific upregulation of SIRT1 (1-2852)-luciferase activity mediated by BRCA1, while TFII-I p70 and TFII-I p46, lacking BRCT-interaction region, had no effect on SIRT1-luciferase activity. TFII-I showed no effect on SIRT1 (1-202)-luciferase activity that lack the binding domain of BRCA1. (**B**) The siRNA-mediated knockdown of BRCA1 decreased the expression of SIRT1. Knockdown of TFII-I also resulted in downregulation of SIRT1. Expression of BRCA1 and p53 was decreased by depletion of TFII-I. HeLa cells were transfected with indicated siRNA. At 48 h after transfection, cells were harvested and analysed by western blotting. (**C**) Chromatin immunoprecipitation assay was performed to confirm the recruitment of BRCA1 and TFII-I at the SIRT1 gene promoter and the p21 gene promoter. Both promoter regions are known to recruit BRCA1.

TFII-I enhances BRCA1-mediated SIRT1 expression

The previous chromatin immunoprecipitation assay showed that BRCA1 interacted with the SIRT1 promoter region between 1354 and 1902 and this binding resulted in elevated expression of SIRT1 (Wang *et al*, 2008; Hiraike *et al*, 2010). We explored whether TFII-I has an effect on the BRCA1-mediated stimulation of the SIRT1 promoter and demonstrated that the BRCA1-mediated stimulation of the SIRT1 promoter was specifically upregulated by exogenous expression of TFII-I although the impact of TFII-I was rather less on SIRT1 promoter compared with AdMLP (Figure 4A, lane 8). The TFII-I p70 and p46 showed no influence to enhance the BRCA1-mediated transactivation of SIRT1-luciferase reporter constructs, but TFII-I ΔN90 showed enhancement on the SIRT1-luciferase transactivation function mediated by BRCA1 (Figure 4, lanes 9–11). The TFII-I *β* was also able to stimulate the SIRT1-luciferase transcriptional activation function mediated by BRCA1 (Figure 4, lane 12). Interaction of BRCA1 with the SIRT1 promoter region was postulated to be important for the activation function of TFII-I because SIRT1-luciferase (1–202) reporter constructs lacking the BRCA1-interaction site showed no enhancement of luciferase activity.

We next examined the effect of siRNA-mediated depletion of TFII-I or BRCA1 on their downstream genes. Knockdown of BRCA1 expression by BRCA1-specific siRNA abrogated the expression of SIRT1 (Figure 4B, lane 3), validating the previous report that the expression of SIRT1 is indeed dependent on BRCA1 (Wang *et al*, 2008). As shown in Figure 4B, lane 2, depletion of the endogenous TFII-I also decreased the expression of SIRT1. Thus, our data demonstrate that TFII-I has a critical role in regulating downstream gene expressions dependent on BRCA1 *in vivo*. Depletion of TFII-I resulted in downregulation of p53 and BRCA1, suggesting a role of TFII-I in DNA damage response (Figure 4B, lane 2).

To test whether TFII-I and BRCA1 were indeed recruited to the SIRT1 promoter, we performed a chromatin immunoprecipitation assay using the SIRT1 gene promoter 1354–1902, a region known to recruit BRCA1 (Wang *et al*, 2008; Hiraike *et al*, 2010) and the p21 gene promoter (Oishi *et al*, 2006). As expected, clear recruitment of endogenous TFII-I and BRCA1 to the target sequence (1354–1902) in the SIRT1 and the p21 promoter was observed in HeLa cells (Figure 4C).

DISCUSSION

The TFII-I is considered to have important roles in regulating the expression of genes as a signal-induced multifunctional transcription factor (Hakre *et al*, 2006; Roy, 2007). Here, we demonstrated that endogenous TFII-I associated with BRCA1, which suggests the possibility that TFII-I has a functional relationship with BRCA1-related phenotypical changes. This interaction between BRCA1 and TFII-I was physiologically functional because our results demonstrated that the TFII-I-containing complex stimulated the autonomous transcriptional activity of BRCT.

The transcriptional activation function of BRCT is considered to be a key to its tumour suppressor activity (Chapman and Verma, 1996; Monteiro *et al*, 1996) because a point mutation within the BRCT domain (A1708E), lacking transactivation function, was shown to be critical for a DNA damage response by the treatment with methylmethane sulfonate (Zhong *et al*, 1999). The importance

of BRCT for transcriptional control and growth suppression is also highlighted by the fact that cancer associated mutations attenuated both, but neutral polymorphism did not (Humphrey *et al*, 1997). The BRCT domain is found in a diverse group of proteins implicated in DNA repair and cell cycle check-point control (Bork *et al*, 1997; Callebaut and Mornon, 1997). BRCA1 carboxyl-terminal domain possesses an autonomous folding unit defined by conserved clusters of hydrophobic amino acids, and BRCT is likely to represent a protein interaction surface (Saka *et al*, 1997). Thus, activation of BRCT has implications both in anti-tumorigenic and in DNA repair processes. Anti-tumorigenic role of TFII-I is also supported by the finding that TFII-I inhibits the growth of MCF-7 (Ogura *et al*, 2006). The study had shown that TFII-I down-regulates a subset of oestrogen-responsive genes, only those containing initiator elements, by recruiting oestrogen receptor α and co-repressors to these promoters. Therefore, TFII-I is not thought to be a general activator of transcription and the transcriptional control by TFII-I would be promoter-dependent manner. The transcriptional regulation played by TFII-I may be complicated because TFII-I was shown to co-immunoprecipitates with transcriptional repressor, histone deacetylase 3 (Wen *et al*, 2003).

We also have shown that TFII-I and BRCA1 colocalise in nuclei of irradiated cells. Previous studies indicated that BRCA1 responds to the repair of DNA by homologous recombination. The BRCA1 associates with RAD51 in subnuclear clusters (Zhong *et al*, 1999). The RAD51 is postulated to be a key component of the mechanism in which DNA damage is repaired by homologous recombination. When cells are exposed to ionising radiation, both BRCA1 and RAD51 localise to the damaged region, and both BRCA1 and RAD51 initiate homologous recombination and the repair of double-strand breaks. Our data that TFII-I and BRCA1 formed nuclear foci after irradiation treatment may suggest that both BRCA1 and TFII-I participates in the DNA damage repair pathway. These data are consistent with the previous observation that TFII-I influences persistence of γ-H2AX foci and thus affects double strand break repair, suggesting a role for TFII-I in DNA repair (Desgranges and Roy, 2006). Our results also indicated that TFII-I promoted BRCA1-dependent transcriptional regulation because SIRT1-luciferase activity was potentiated by the ectopic expression of TFII-I. The TFII-I would serve as a transcriptional activation factor to manipulate transcriptions, thereby influencing transcriptional products such as SIRT1. These results also suggest the possible mechanism how TFII-I regulates DNA damage machinery because SIRT1 possesses DNA repair activity (Jeong *et al*, 2007). In consistent with these data, depletion of endogenous TFII-I resulted in a decreased expression of p53 and BRCA1. We have to further confirm the effect of DNA damage response when TFII-I is abrogated to show its involvement in this mechanism. Our results showed a new insight that TFII-I may serve, at least in part, as DNA damage response machinery.

In conclusion, our data indicate that TFII-I have an important role in regulating BRCA1-mediated functions through binding to the BRCT domain and it may be probable that TFII-I is involved in anti-tumorigenic processes. The meaning of TFII-I functions would be apparent by evaluating its expression in tumour tissues such as breast cancer. The expression of TFII-I would be therapeutically beneficial by affecting different TFII-I-mediated regulatory pathways together with BRCA1 and the failure of binding between BRCA1 and TFII-I may be a key event in cancer predisposition.

ACKNOWLEDGEMENTS

This study was supported by a Grant-in-Aid for Scientific Research from the Ministry of Education, Science and Culture, JMS Bayer Schering Pharma Grant, and Kowa Life Science Foundation, Japan. We thank Dr RG Roeder (The Rockefeller University) for TFII-I expression vectors and Dr AL Roy (Tufts University School of Medicine) for TFII-I expression vectors and deletion mutants.

REFERENCES

Anderson SF, Schlegel BP, Nakajima T, Wolpin ES, Parvin JD (1998) BRCA1 protein is linked to the RNA polymerase II holoenzyme complex via RNA helicase A. *Nat Genet* **3:** 254–256

Bork P, Hofmann K, Bucher P, Neuwald AF, Altschul SF, Koonin EV (1997) A superfamily of conserved domains in DNA damage-responsive cell cycle checkpoint proteins. *FASEB J* **11:** 68–76

Callebaut I, Mornon JP (1997) From BRCA1 to RAP1: a widespread BRCT module closely associated with DNA repair. *FEBS Lett* **400:** 25–30

Chapman MS, Verma IM (1996) Transcriptional activation by BRCA1. *Nature* **382:** 678–679

Cheriyath V, Roy AL (2001) Structure-function analysis of TFII-I. Roles of the N-terminal end, basic region, and I-repeats. *J Biol Chem* **276:** 8377–8383

Desgranges ZP, Roy AL (2006) TFII-I: connecting mitogenic signals to cell cycle regulation. *Cell Cycle* **5:** 356–359

Hakre S, Tussie-Luna MI, Ashworth T, Novina CD, Settleman J, Sharp PA, Roy AL (2006) Opposing functions of TFII-I spliced isoforms in growth factor-induced gene expression. *Mol Cell* **24:** 301–308

Hiraike H, Wada-Hiraike O, Nakagawa S, Koyama S, Miyamoto Y, Sone K, Tanikawa M, Tsuruga T, Nagasaka K, Matsumoto Y, Oda K, Shoji K, Fukuhara H, Saji S, Nakagawa K, Kato S, Yano T, Taketani Y (2010) Identification of DBC1 as a transcriptional repressor for BRCA1. *Br J Cancer* **102:** 1061–1067

Hohenstein P, Kielman MF, Breukel C, Bennett LM, Wiseman R, Krimpenfort P, Cornelisse C, van Ommen GJ, Devilee P, Fodde R (2001) A targeted mouse Brca1 mutation removing the last BRCT repeat results in apoptosis and embryonic lethality at the headfold stage. *Oncogene* **20:** 2544–2550

Humphrey JS, Salim A, Erdos MR, Collins FS, Brody LC, Klausner RD (1997) Human BRCA1 inhibits growth in yeast: potential use in diagnostic testing. *Proc Natl Acad Sci USA* **94:** 5820–5825

Jeong J, Juhn K, Lee H, Kim SH, Min BH, Lee KM, Cho MH, Park GH, Lee KH (2007) SIRT1 promotes DNA repair activity and deacetylation of Ku70. *Exp Mol Med* **39:** 8–13

Monteiro AN, August A, Hanafusa H (1996) Evidence for a transcriptional activation function of BRCA1 C-terminal region. *Proc Natl Acad Sci USA* **93:** 13595–13599

Moynahan ME, Chiu JW, Koller BH, Jasin M (1999) Brca1 controls homology-directed DNA repair. *Mol Cell* **4:** 511–518

Ogura Y, Azuma M, Tsuboi Y, Kabe Y, Yamaguchi Y, Wada T, Watanabe H, Handa H (2006) TFII-I down-regulates a subset of estrogen-responsive genes through its interaction with an initiator element and estrogen receptor alpha. *Genes Cells* **11:** 373–381

Oishi H, Kitagawa H, Wada O, Takezawa S, Tora L, Kouzu-Fujita M, Takada I, Yano T, Yanagisawa J, Kato S (2006) An hGCN5/TRRAP histone acetyltransferase complex co-activates BRCA1 transactivation function through histone modification. *J Biol Chem* **281:** 20–26

Pober BR (2010) Williams-Beuren syndrome. *N Engl J Med* **362:** 239–252

Roy AL (2007) Signal-induced functions of the transcription factor TFII-I. *Biochim Biophys Acta* **1769:** 613–621

Roy AL, Du H, Gregor PD, Novina CD, Martinez E, Roeder RG (1997) Cloning of an inr- and E-box-binding protein, TFII-I, that interacts physically and functionally with USF1. *EMBO J* **16:** 7091–7104

Saka Y, Esashi F, Matsusaka T, Mochida S, Yanagida M (1997) Damage and replication checkpoint control in fission yeast is ensured by interactions of Crb2, a protein with BRCT motif, with Cut5 and Chk1. *Genes Dev* **11:** 3387–3400

Genetics and Genomics

Scully R, Ganesan S, Vlasakova K, Chen J, Socolovsky M, Livingston DM (1999) Genetic analysis of BRCA1 function in a defined tumor cell line. *Mol Cell* 4: 1093 - 1099

Wada O, Oishi H, Takada I, Yanagisawa J, Yano T, Kato S (2004) BRCA1 function mediates a TRAP/DRIP complex through direct interaction with TRAP220. *Oncogene* 23: 6000 - 6005

Wang RH, Zheng Y, Kim HS, Xu X, Cao L, Luhasen T, Lee MH, Xiao C, Vassilopoulos A, Chen W, Gardner K, Man YG, Hung MC, Finkel T, Deng CX (2008) Interplay among BRCA1, SIRT1, and Survivin during BRCA1-associated tumorigenesis. *Mol Cell* 32: 11 - 20

Wen YD, Cress WD, Roy AL, Seto E (2003) Histone deacetylase 3 binds to and regulates the multifunctional transcription factor TFII-I. *J Biol Chem* 278: 1841 - 1847

Zhong Q, Chen CF, Li S, Chen Y, Wang CC, Xiao J, Chen PL, Sharp ZD, Lee WH (1999) Association of BRCA1 with the hRad50-hMre11-p95 complex and the DNA damage response. *Science* 285: 747 - 750

β-catenin (*CTNNB1*) S33C Mutation in Ovarian Microcystic Stromal Tumors

Daichi Maeda, MD, PhD, Junji Shibahara, MD, PhD,* Takahiko Sakuma, MD, PhD,† Masanori Isobe, MD,‡ Shinichi Teshima, MD,§ Masaya Mori, MD,‖ Katsutoshi Oda, MD, PhD,¶ Shunsuke Nakagawa, MD, PhD,¶ Yuji Taketani, MD, PhD,¶ Shumpei Ishikawa, MD, PhD,* and Masashi Fukayama, MD, PhD**

Abstract: Microcystic stromal tumor (MCST) is a recently described subtype of ovarian tumor characterized by prominent microcystic histologic pattern and diffuse immunoreactivity for CD10 and vimentin. However, its pathobiology, particularly its histogenesis, remains largely unclear. Here, we report 2 cases of ovarian MCST, in which we have performed extensive histologic, immunohistochemical, and genetic investigations to determine its distinct nature among ovarian neoplasms. The patients were 32 and 41 years of age. Both tumors were solid and cystic masses involving the right ovary. Microscopically, tumor cells with generally bland, round-to-ovoid nuclei grew in microcystic, macrocystic, and solid patterns. Intervening thick fibrous stroma was observed. Immunohistochemically, tumor cells were diffusely and strongly positive for CD10, vimentin, and Wilms tumor 1. Furthermore, we detected aberrant nuclear expression of β-catenin protein in both cases. Of interest, mutation analyses revealed the presence of an identical point mutation, c.98C > G, in exon 3 of β-catenin (*CTNNB1*) in both tumors. This is an oncogenic mutation that causes replacement of serine with cysteine at codon 33, leading to the loss of a phosphorylation site in the β-catenin protein. The results of this study strongly suggest that dysregulation of the Wnt/β-catenin pathway plays a fundamental role in the pathogenesis of ovarian MCST. Finally, by comparing the immunophenotype of MCST with its histologic mimics and other ovarian sex cord-stromal tumors, we were able to identify unique features of MCST and a panel of markers useful in differential diagnosis.

From the *Department of Pathology, Graduate School of Medicine; ¶Department of Obstetrics and Gynecology, Faculty of Medicine, The University of Tokyo; §Department of Pathology, Doai Memorial Hospital; ‖Department of Pathology, Mitsui Memorial Hospital, Tokyo; †Department of Diagnostic Pathology; and ‡Department of Obstetrics and Gynecology, Osaka Rosai Hospital, Sakai, Japan.

Conflicts of Interest and Source of Funding: The authors have disclosed that they have no significant relationships with, or financial interest in, any commercial companies pertaining to this article. This study was supported by a Grant-in-Aid for Scientific Research (KAKENHI) from the Japan Society for the Promotion of Science.

Correspondence: Masashi Fukayama, MD, PhD, Department of Pathology, Graduate School of Medicine, The University of Tokyo, 7-3-1 Hongo Bunkyoku, Tokyo 113-0033, Japan (e-mail: mfukayama-tky@umin.net).

Key Words: microcystic stromal tumor, ovary, β-catenin

(*Am J Surg Pathol* 2011;35:1429–1440)

In 2009, Irving and Young[7] reported a series of ovarian neoplasms that they described as "superficially reminiscent of thecoma in some regions, but with a microcystic pattern often so conspicuous that it dwarfed the thecoma-like regions." On the basis of the distinctive histologic and immunohistochemical features of these tumors, the researchers designated the tumors as a "microcystic stromal tumor" (MCST), which is a novel entity. In their report of 16 cases, the tumors were characterized by the principal microscopic appearance of microcysts, with variably prominent solid cellular areas and fibrous stroma. Diffuse and strong expressions of vimentin and CD10 were also noted. Their precise origin and background genetic alterations remain unclear. However, a stromal nature was favored in the article because of the morphologic resemblance to thecoma and by exclusion of other possibilities.

We recently encountered 2 cases of ovarian MCSTs that exhibited features similar to those reported. In this study, we attempted to further clarify the histologic, immunohistochemical, and genetic features of this unique ovarian neoplasm. We found a previously undescribed "macrocystic pattern" of tumor growth in both MCSTs, along with microcystic and solid patterns. In addition, we recognized a certain degree of morphologic resemblance, particularly in the cellular features, between ovarian MCSTs and pancreatic solid pseudopapillary neoplasms (SPNs). The finding that CD10 and vimentin are both commonly expressed in ovarian MCSTs[7] and pancreatic SPNs[14] was also of interest. These notions have led us to investigate β-catenin alteration in ovarian MCSTs, as pancreatic SPN is well known for harboring a β-catenin mutation.[1,24] Using immunohistochemical analyses, we found that aberrant nuclear accumulation of β-catenin protein occurs in MCSTs. By direct sequencing, we then showed that both tumors harbored an oncogenic somatic mutation in exon 3 of the β-catenin (*CTNNB1*) gene.

Further, we compared the morphology and immunohistochemical profiles of ovarian MCSTs and other

ovarian tumors that can be differentially diagnosed, such as sex cord-stromal tumors, struma ovarii (SO), and yolk sac tumors (YSTs). Among the ovarian tumors, granulosa cell tumor (GCT), along with thecoma, is one of the top differential diagnoses of MCST. By immunohistochemistry we showed that MCSTs do not express sex cord-stromal markers α-inhibin and calretinin, which are frequently positive in GCTs and thecomas. To strictly rule out the possibility that ovarian MCST was a variant of GCT, we also sequenced *FOXL2*, a gene mutated in nearly all ovarian GCTs.[2,8,10,20,21] As neither of the MCSTs harbored the *FOXL2* mutation, we concluded that MCST is a tumor that can be clearly distinguished from the GCT lineage. The ovarian counterpart of pancreatic SPN (ovarian SPN), which was recently reported,[5] is another important entity that requires distinction from MCSTs. As we were unable to identify a case of ovarian SPN, we included pancreatic SPNs in the series of cases assessed for immunophenotypes and attempted to show the difference between MCSTs and SPNs.

To our knowledge, this is the first report describing genetic alterations in MCST. Distinct histologic and immunohistochemical properties of MCST, along with its differential diagnosis, are presented in detail.

MATERIALS AND METHODS

Tissue Samples

We retrieved and reviewed hematoxylin and eosin-stained sections of 2 cases of ovarian MCST. The ovarian tumor in case 1 was surgically removed at the University of Tokyo Hospital, and its pathologic diagnosis was made by 2 of the authors (D.M. and J.S.) on the basis of 17 sections taken from the tumor. Case 2 was from Osaka Rosai Hospital and was retrieved from the consultation files of 1 of the authors (D.M.). Twenty-two slide sections were reviewed for the ovarian tumor in case 2. Neither of the cases was reported previously. The diagnosis of MCST was made on the basis of the criteria proposed by Irving and Young.[7] The tumors were required to exhibit the following features: (1) a microcystic pattern and regions with lobulated cellular masses with intervening, sometimes hyalinized, fibrous stroma, (2) absence of morphologic features enabling any other specific diagnosis in the sex cord-stromal category, (3) absence of epithelial elements, and (4) absence of teratomatous or other germ cell elements. Clinical information was obtained from the clinicians and hospital charts for each case.

In addition, we studied a broad range of ovarian neoplasms that may be included in the differential diagnosis of MCST. The following tumors were retrieved from the archives of the Departments of Pathology of the University of Tokyo and Mitsui Memorial Hospital: 11 adult granulosa cell tumors (AGCTs), 2 juvenile granulosa cell tumors (JGCTs), 11 fibromas, 4 thecomas, 4 fibrothecomas, 2 Sertoli-Leydig cell tumors, 2 stromal tumors with minor sex cord elements, 1 steroid cell tumor, 1 gonadoblastoma, 7 SO, and 8 YSTs. We also retrieved 3 pancreatic SPNs to examine the similarities and differences between ovarian MCSTs and pancreatic SPNs.

Immunohistochemistry

All the tissue samples were fixed in formalin and embedded in paraffin. Full tissue sections (4-μm thick) were used for immunohistochemistry in all cases. Immunohistochemical staining was performed according to standard techniques on a Ventana Benchmark XT autostainer (Ventana Medical Systems Inc., Tucson, AZ). Appropriate positive and negative controls were included. A list of antibodies used in this study and criteria for positive immunoreactivity for each antibody are shown in Table 1.

DNA Extraction and Gene Sequencing of CTNNB1 and FOXL2

We analyzed cases of ovarian MCST for *CTNNB1* and *FOXL2* mutations. Sections (8-μm to 10-μm thick) were cut from paraffin-embedded blocks containing MCSTs and those containing background tubal tissues from the same patients. Representative areas of the sections were macrodissected. Extraction of genomic DNA was performed using a PicoPure DNA Extraction Kit (Life Technologies Corp., Carlsbad, CA). Exon 3 of *CTNNB1*, the gene encoding β-catenin, contains the region involved in glycogen synthase kinase 3β phosphorylation. This exon was amplified using the following primer pairs: F: 5′-GATTTGATGGAGTTGGACATG G-3′ and R: 5′-GCTACTTGTTCTTGAGTGAAGG-3′. A somatic mutation in the *FOXL2* gene was reported to be present in almost all (86 of 89, 97%) morphologically defined AGCTs.[2,8,10,11,20,21] This *FOXL2* c.402C > G mutation changes a highly conserved cysteine residue to a tryptophan (p.C134W). We amplified exon 1 of *FOXL2*, which contains the above mutation, using the following set of primers: F: 5′-CCGCCACAACCTCAGCCTC-3′ and R: 5′-CGCCGGTAGTTGCCCTTCTC-3′. An Applied Biosystems 3730xl DNA Analyzer and 3130xl Genetic Analyzer were used for sequence analysis.

This study was approved by the institutional review boards of the facilities involved.

RESULTS

Clinical Features of Ovarian MCSTs

Case 1

A 33-year-old woman, gravida 0, para 0, with no particular relevant past history was found to have a right ovarian mass and multiple uterine masses. The ovarian mass showed a predominantly solid and partially cystic appearance on a computed tomographic scan, which raised the possibility of a sex cord-stromal tumor. The uterine masses were diagnosed clinically as leiomyomas. The patient initially received a gonadotropin-releasing hormone analog. After treatment, the uterine tumors decreased in size. However, the right ovarian tumor grew larger. Serum lactose dehydrogenase was elevated at 381 IU/L (normal range, 125 to 237 IU/L). Tumor markers, such as carcinoembryonic antigen, CA19-9,

TABLE 1. Antibodies Used for Immunohistochemistry and Criteria for Positive Immunoreactivity

Antibody	Dilution	Clone	Manufacturer	Criteria for Positive Immunoreactivity
CD10	1:200	NCL-CD10-270	Novocastra	Cytoplasmic or membranous staining in > 5% of tumor cells
Vimentin	1:1000	V9	Dako	Cytoplasmic or membranous staining in > 5% of tumor cells
WT-1	1:25	6F-H2	Dako	Nuclear staining in > 50% of tumor cells
β-Catenin	1:2000	14/Beta-Catenin	BD Biosciences	Nuclear staining in > 50% of tumor cells
α-Inhibin	1:50	R1	Dako	Cytoplasmic staining in > 5% of tumor cells
Calretinin	1:25	NCL-Calretinin	Novocastra	Cytoplasmic or membranous staining in > 5% of tumor cells
ER	Prediluted	SP1	Ventana	Nuclear staining in > 50% of tumor cells
PgR	Prediluted	IE2	Ventana	Nuclear staining in > 50% of tumor cells
EMA	1:100	E29	Dako	Membranous staining in > 5% of tumor cells
Cytokeratin (AE1/AE3)	1:100	AE1/AE3	Dako	Cytoplasmic or membranous staining in > 5% of tumor cells
Cytokeratin (Cam 5.2)	Prediluted	Cam 5.2	BD Biosciences	Cytoplasmic or membranous staining in > 5% of tumor cells
Cytokeratin 7	1:100	OV-TL 12/30	Dako	Cytoplasmic or membranous staining in > 5% of tumor cells
CD56	1:50	NCL-CD56-1B6	Novocastra	Membranous staining in > 5% of tumor cells
Synaptophysin	1:100	Poly	Dako	Cytoplasmic staining in > 5% of tumor cells
Chromogranin A	1:200	Poly	Dako	Cytoplasmic staining in > 5% of tumor cells
Desmin	1:100	D33	Dako	Cytoplasmic staining in > 5% of tumor cells
Smooth muscle actin	1:400	1A4	Dako	Cytoplasmic staining in > 5% of tumor cells
CD34	1:20	My10	Becton Dickinson	Cytoplasmic or membranous staining in > 5% of tumor cells
CD31	1:40	JC70A	Dako	Cytoplasmic or membranous staining in > 5% of tumor cells
D2-40	1:60	D2-40	Covance	Cytoplasmic or membranous staining in > 5% of tumor cells
CD99	1:100	12E7	Dako	Membranous staining in > 5% of tumor cells
TTF-1	1:200	8G7G3/1	Dako	Nuclear staining in > 5% of tumor cells
AFP	1:1000	Poly	Dako	Cytoplasmic or membranous staining in > 5% of tumor cells
Ki-67	1:100	MIB-1	Dako	Percentage of tumor cells showing positive nuclear immunoreactivity was calculated as MIB-1 index.

AFP indicates α-fetoprotein; EMA, epithelial membrane antigen; ER, estrogen receptor; PgR, progesterone receptor; TTF-1, thyroid transcription factor 1.

and CA125, were within the respective normal ranges. To make definitive diagnoses of ovarian and uterine tumors, the patient underwent right adnexectomy, enucleation of the uterine masses, and partial omentectomy. The patient is currently free of disease 14 months after surgery.

Case 2

A 41-year-old woman presented with lower abdominal pain. Ultrasonography revealed an ovarian mass. On a computed tomographic scan, the mass was a multilocular cystic lesion that showed mild contrast enhancement. Radiographically, an ovarian mucinous adenocarcinoma was suspected. The patient underwent a right adnexectomy and enucleation of a uterine leiomyoma. The patient is currently free of disease 4 months after surgery.

Gross Features of Ovarian MCSTs

Case 1

The right ovarian tumor measured 11.5 × 6.5 × 5.0-cm. It was confined in the ovary, and the surface of the ovary was smooth. Cut surfaces of the tumor revealed a mixed solid and cystic appearance (Fig. 1A). Solid areas were predominantly whitish. Areas with hemorrhagic change were also observed.

Case 2

The right ovarian tumor weighed 340 g and measured 9.5 cm in maximum diameter. The ovarian surface of the ovary was smooth. Cut surfaces of the tumor revealed a prominent spongy appearance with numerous cystic cavities filled with blood (Fig. 1B). Solid and white areas were also found.

Histologic Features of Ovarian MCSTs

The histologic features of the tumor in case 1 (Fig. 2) and case 2 (Fig. 3) were quite similar. Both tumors were surrounded by fibrous capsules and were well demarcated from the background ovarian parenchyma. A thin layer of ovarian medulla with vascular networks was present on the outer rim of the tumor, and the ovarian cortex was observed circumferentially toward the surface of the ovary. The ovarian cortex was particularly well preserved in the tumor of case 2. Many follicles were observed around the tumor. The principal structural patterns that tumor cells of MCSTs exhibited included a microcystic pattern, a solid pattern, and a macrocystic pattern. The presence of intervening thick fibrous stroma was another feature that characterized MCSTs. The fibrous stroma frequently showed hyalinization. Occasional myxoid change was also seen in the stroma. Areas of hemorrhage with hemosiderin deposition were present within both tumors.

In case 1, solid and microcystic areas predominated, and the macrocystic pattern was seen in a scattered manner. Macrocystic structures were predominant in case 2, and they were easily identifiable on low-power examination. A gradual transition between solid areas, microcystic areas, and macrocystic areas was frequently seen. The tumor occasionally showed a reticular appearance in the areas where irregularly shaped cysts of

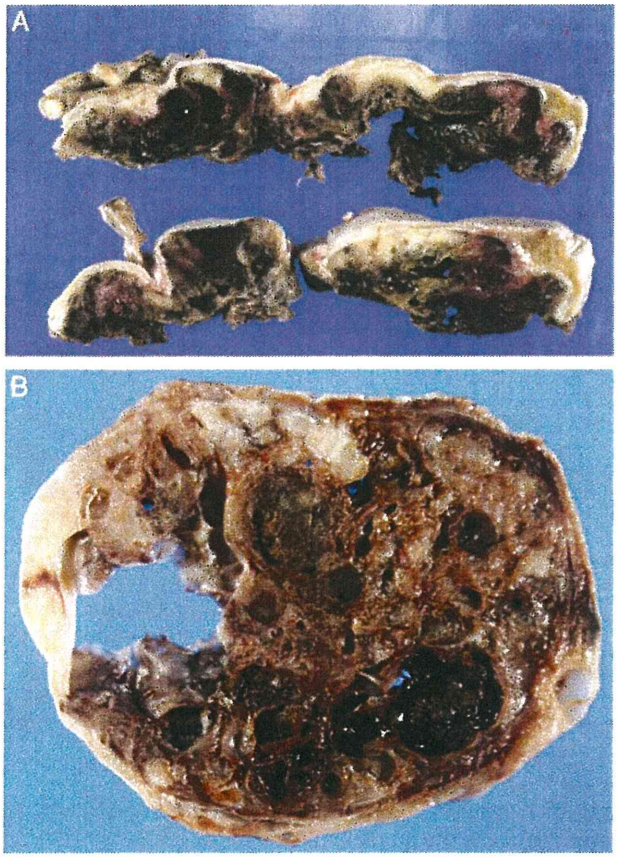

FIGURE 1. Gross pictures of ovarian MCST. A, Case 1. Cut section of the tumor showed solid and white areas admixed with numerous cystic lumens. Marked hemorrhagic changes were seen. B, Case 2. The cut surface of the tumor revealed a characteristic sponge-like appearance. Many of the cystic cavities were filled with bloody content. Whitish solid components were also present in the tumor.

variable sizes anastomosed with each other. The lumens of microcysts or macrocysts were filled with eosinophilic exudative content, myxoid content, or blood. Marked congestive changes were found in the tumor of case 2, and many of the cystic spaces lined by the tumor cells were filled with blood. These congestive areas gave a "hemangiomatous" or "hemangiopericytomatous" impression. Although many of the microcysts and macrocysts were lined by tumor cells, epithelial glandular differentiation was not evident in either of the tumors. Pseudopapillary architecture was absent in both tumors.

Individual tumor cells had round-to-ovoid and sometimes short-spindled nuclei with very fine chromatin. Nucleoli were inconspicuous or very small when present. Most of the neoplastic cells had a faintly eosinophilic cytoplasm. In general, tumor cell nuclei were monotonous and bland. However, in case 2, neoplastic cells with enlarged nuclei and abundant eosinophilic cytoplasm were observed focally in $< 1\%$ of the tumor. Some of these cells mimicked luteinized cells. Mitoses were hardly detected in either tumor (average: 0 mitoses/10 high-power field).

Immunophenotypes of Ovarian MCSTs, Other Ovarian Tumors, and Pancreatic SPNs

The 2 ovarian MCSTs examined in this study showed quite similar immunophenotypes. Diffuse and strong immunoreactivity for vimentin (Fig. 4A) and CD10 (Fig. 4B) was observed in both cases. In addition, we found that these tumors commonly showed diffuse and strong nuclear immunoreactivity for β-catenin (Fig. 5A) and Wilms tumor 1 (WT-1) (Fig. 4C). MCSTs were completely negative for sex cord markers (α-inhibin and calretinin), hormone receptors (estrogen receptor and progesterone receptor), neuroendocrine markers (CD56, synaptophysin, and chromogranin A), vascular markers (CD31, CD34, and D2-40), and mesenchymal markers including desmin and smooth muscle actin. Other negative markers included CD99, thyroid transcription factor-1, α-fetoprotein, SALL4, epithelial membrane antigen, cytokeratin (Cam 5.2), and cytokeratin 7. MCST in case 1 was completely negative for cytokeratin (AE1/AE3). However, approximately 20% of the tumor cells in case 2 showed positive immunoreactivity for cytokeratin (AE1/AE3) (Fig. 4D). Ki-67-labeling index (MIB-1 index) was 7% and 10% in case 1 and case 2, respectively.

Immunophenotypes of ovarian MCSTs, other ovarian tumors that can exhibit similar morphologic features, such as sex cord-stromal tumors, SOs, and YSTs, and pancreatic SPNs, are summarized in Table 2. Among the ovarian tumors examined, aberrant nuclear accumulation of β-catenin was specifically observed in MCSTs (Figs. 6B–E). Two of 3 pancreatic SPNs showed nuclear immunoreactivity for β-catenin (Fig. 6F). Vimentin was expressed in most ovarian sex cord-stromal tumors. In contrast, CD10 positivity was rarely observed in ovarian sex cord-stromal tumors, YSTs, or SOs. Although WT-1 expression was commonly observed in various kinds of ovarian sex cord-stromal tumors, including GCTs, fibromas, thecomas, and Sertoli-Leydig cell tumors, their immunoreactivity was usually neither as strong nor as diffuse in comparison with WT-1 expression in MCSTs. α-Inhibin, which is frequently expressed in ovarian sex cord-stromal tumors, was not expressed in MCSTs. The pancreatic SPNs were positive for CD10 and vimentin. However, we observed a significant difference in the immunophenotypes of MCSTs and SPNs, with MCSTs showing a $WT\text{-}1^{+}/PgR^{-}/CD56^{-}$ pattern and SPNs showing a $WT\text{-}1^{-}/PgR^{+}/CD56^{+}$ pattern.

Mutation Analyses of β-catenin (CTNNB1) and FOXL2 in MCSTs

Both cases of ovarian MCST had the same oncogenic missense mutations of *CTNNB1*, which is the gene encoding β-catenin (Fig. 4). The mutations detected were both c.98C > G mutations that cause replacement of serine with cysteine at codon 33. Mutations in exon 1 of *FOXL2* were not detected in MCSTs.

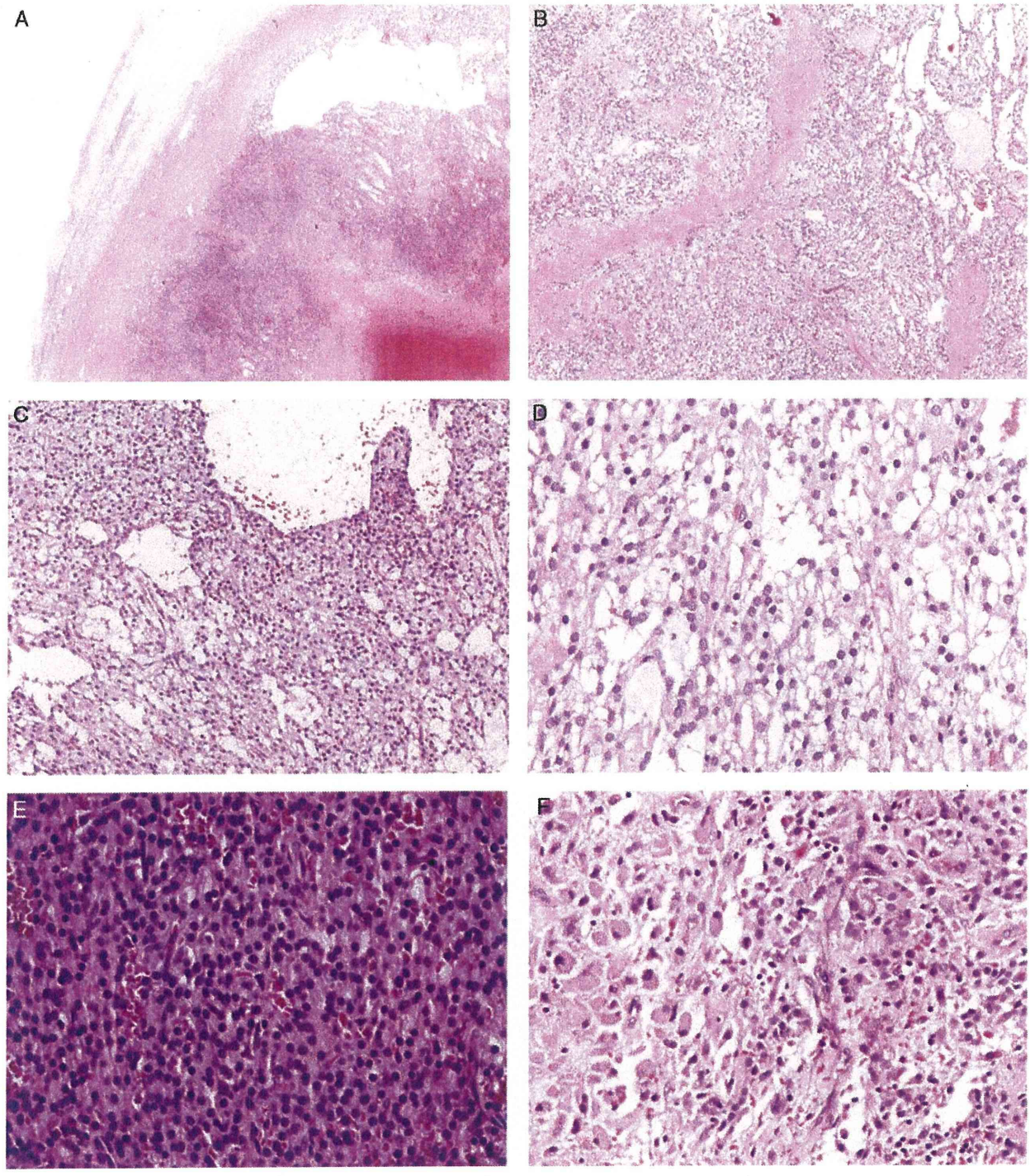

FIGURE 2. Histology of ovarian MCST in case 1. A, Low-power view of the tumor. The tumor was a well-demarcated lesion with a fibrous capsule. Marked hemorrhage was observed in its center. B, Thick fibrous stroma was seen between areas of tumor cell growth. C, Tumor cells formed cysts of various sizes. A mixture of microcystic and macrocystic structures was observed. D, Representative high-power view of the tumor. Monotonous and bland tumor cells with round-to-ovoid nuclei grew in a microcystic pattern. E, A solid pattern of growth was seen in parts. F, Some tumor cells had abundant eosinophilic cytoplasm.

DISCUSSION

In this study, we describe the histopathologic features of ovarian MCSTs in detail. Although the number of cases we studied was not large, their unique and impressive histology and homologous immunophenotype convinced us of their distinct nature among

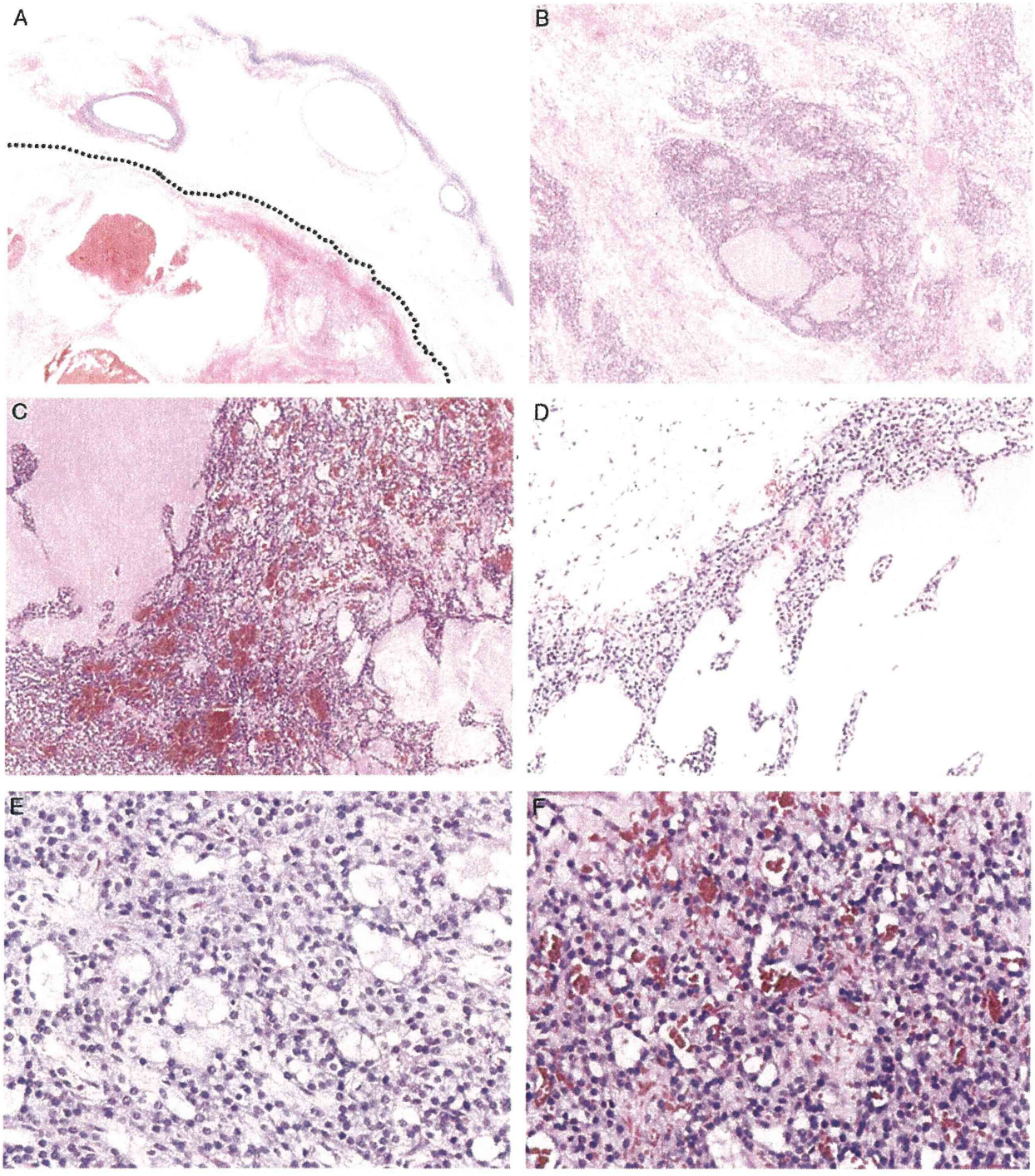

FIGURE 3. Histology of ovarian MCST in case 2. A, Low-power view of the tumor border (dotted line). A thin layer of ovarian medulla was seen surrounding the tumor. The ovarian cortex was well preserved, and numerous follicles could be seen. B, Tumor cell nests and intersecting fibrous stroma. C, The tumor cells grew in macrocystic and microcystic patterns. Marked congestion was observed. D, The wall of the macrocystic space was lined with irregularly shaped nests of tumor cells. E, Representative high-power view of the tumor. Cells with minimum cytologic atypia grew in microcystic and solid patterns. F, Hemangiomatous component of the tumor. The cystic lumens were filled with blood.

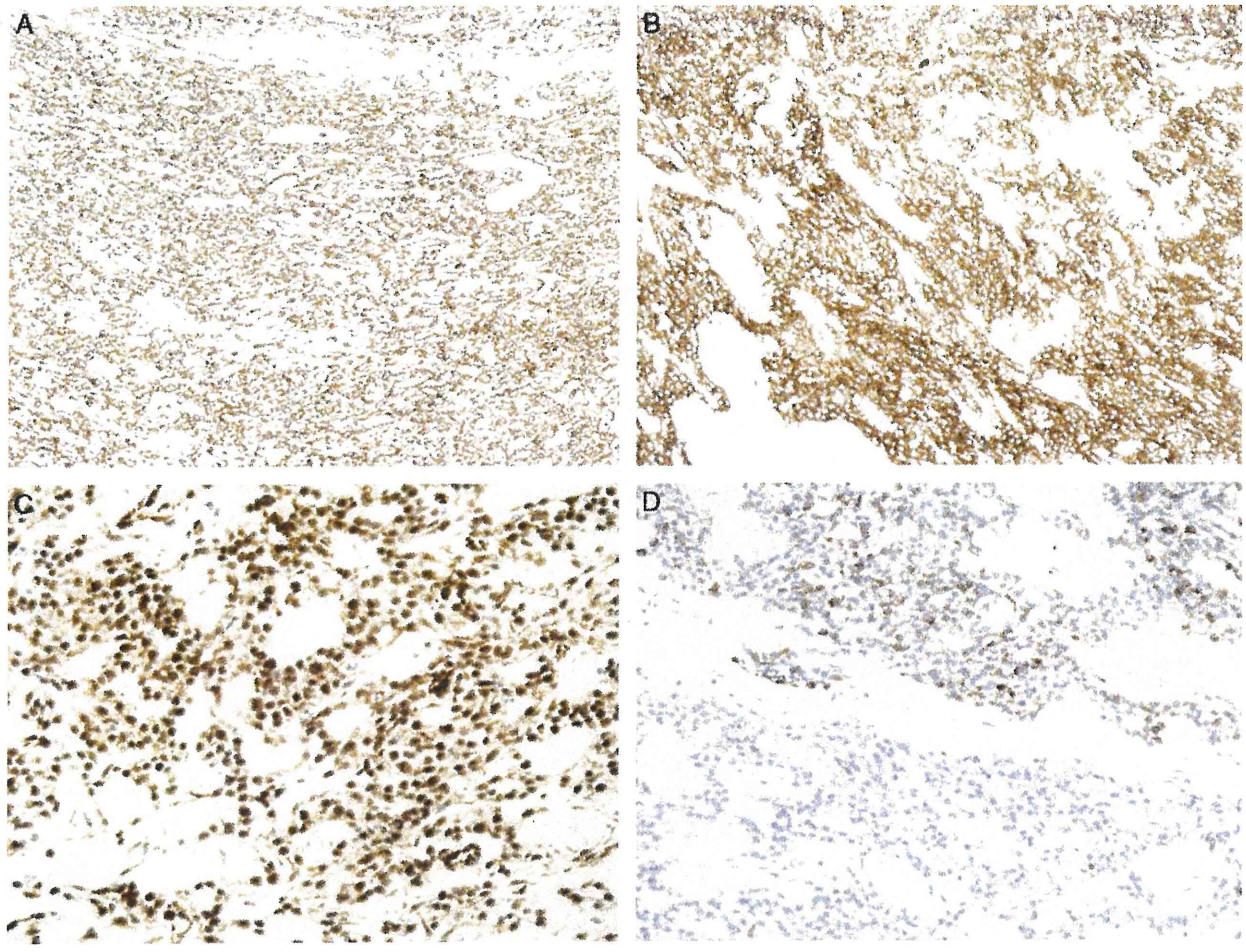

FIGURE 4. Immunohistochemical features of ovarian MCSTs. Both cases of ovarian MCSTs showed diffuse and strong positivity for (A) vimentin, (B) CD10, and (C) WT-1. D. In case 2, the tumor showed focal staining for cytokeratin (AE1/AE3).

ovarian neoplasms and prompted us to further investigate their pathogenesis.

Macroscopically, ovarian MCSTs in our series commonly showed a "solid and cystic" or "sponge-like" appearance. In a previously reported series,[7] 11 of 16 MCSTs showed a solid and cystic gross appearance, and 2 cases were predominantly cystic. Thus, we believe that a "solid and cystic" gross appearance is one of the key features of MCSTs.

Histologically, the following features appear to be characteristic of MCSTs:

1. Mixture of microcystic, macrocystic, and solid structures.
2. Presence of intervening thick fibrous stroma.
3. Growth of monotonous tumor cells with round-to-ovoid and generally bland nuclei with very fine chromatin.
4. Well-demarcated tumor borders.
5. Focal areas of congestive and hemorrhagic change that can give a hemangiomatous impression.

In a previous report,[7] the researchers primarily focused on the microcystic pattern as the characteristic structural pattern of MCSTs. The microcystic feature was observed in all of their cases and was regarded as the most striking morphologic characteristic. This was the main reason why they included "microcystic" in the nomenclature when proposing this new and unique ovarian tumor entity. Along with the microcystic pattern, a solid pattern of tumor cell growth was described in their report. Notably, microcystic components were relatively minor in some of their cases. In our cases, the tumors were composed mainly of 3 major structural patterns: "microcystic," "macrocystic," and "solid." Although the macrocystic structure was not described in the previous series, it was commonly observed in our cases and was predominant in 1 case. Therefore, we believe that it should be listed as one of the major structural patterns that MCSTs exhibit. At this point, it is unclear how microcysts and macrocysts are formed in MCSTs. Whether it is the nature of tumor cells to form cysts, or cystic spaces are the consequence of degenerative changes, is unknown. Many of the cystic spaces are, in fact, lined by tumor cells. However, epithelial glandular differentiation (glands formed by cuboidal cells or columnar cells)

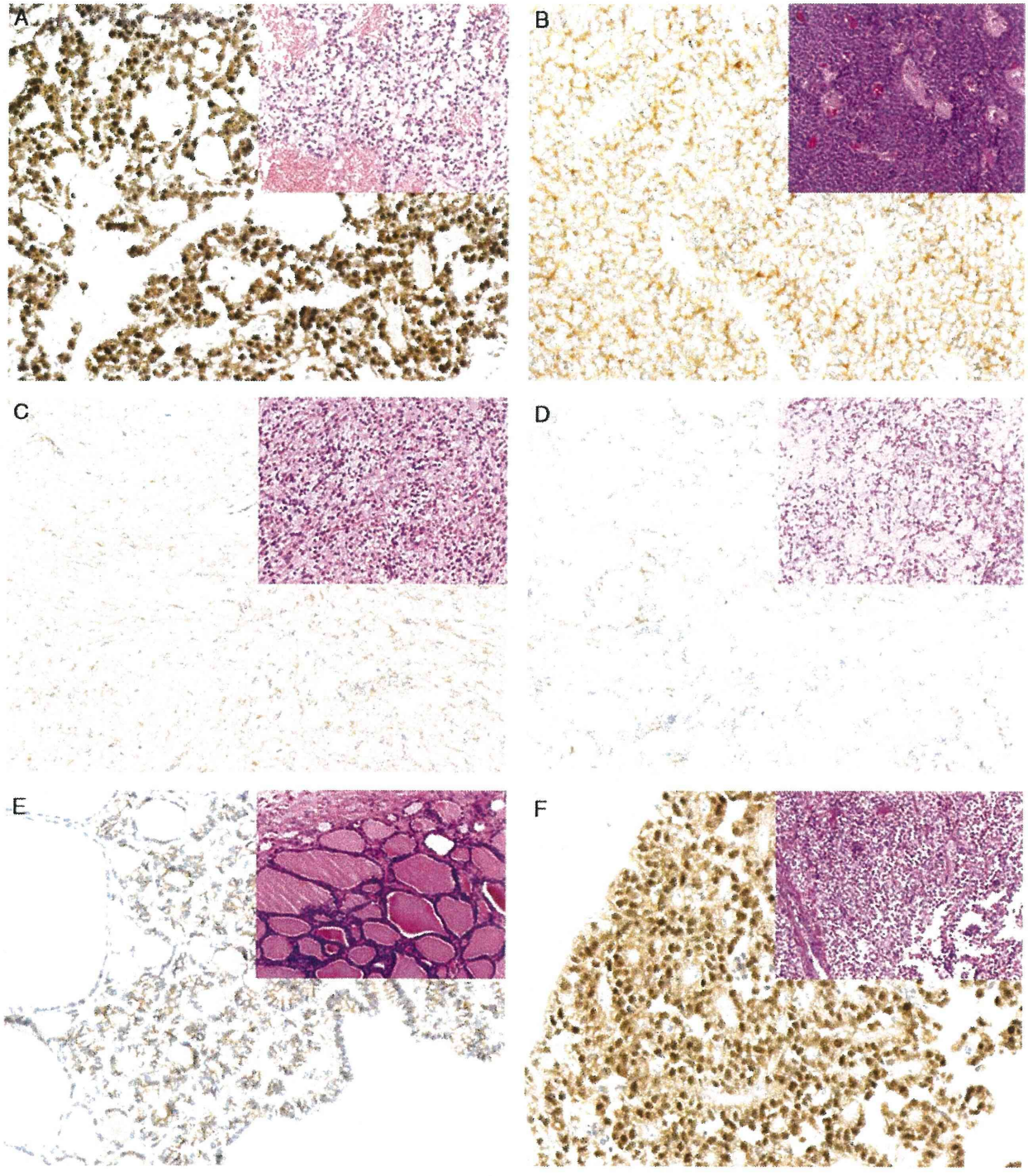

FIGURE 5. Immunohistochemical detection of β-catenin protein in ovarian (A) MCST, (B) AGCT, (C) thecoma, (D) YST, (E) SO, and (F) pancreatic solid pseudopapillary tumor. Among the ovarian tumors examined in this series, diffuse nuclear accumulation of β-catenin protein was observed only in MCST. Pancreatic SPN showed a similar expression pattern.

was not observed in any areas of the tumor. A gradual transition between solid, microcystic, and macrocystic areas was observed, and contents of the cystic lumen differed significantly from exudative, myxoid, to bloody. On the basis of these findings, we speculate that stromal alteration caused by tumor cell secretion or degenerative changes due to processes such as edema and congestion play a role in the formation of variably sized cystic lumens in MCSTs.

In addition to the above described structural patterns, the nuclear features of MCSTs are also

TABLE 2. Results of Immunohistochemistry in Ovarian MCSTs, Other Ovarian Tumors, and Pancreatic SPNs

	Ovary						Pancreas
	MCST	GCT	F/T/FT	Other SCST	YST	SO	SPN
β-Catenin	2/2	0/13	0/19	0/6	0/8	0/7	2/3
CD10	2/2	0/13	1/19	2/6	1/8	2/7	3/3
Vimentin	2/2	13/13	19/19	6/6	6/8	7/7	3/3
WT-1	2/2	8/13	15/19	2/6	0/8	0/7	0/3
α-Inhibin	0/2	12/13	7/19	6/6			
TTF-1	0/2					7/7	
SALL4	0/2				8/8		
AFP	0/2				8/8		
PgR	0/2						3/3
CD56	0/2						3/3

AFP indicates α-fetoprotein; F, fibroma; FT, fibrothecoma; PgR, progesterone receptor; SCST, sex cord-stromal tumor; T, thecoma; TTF-1, thyroid transcription factor 1.

characteristic. The nuclei are round to ovoid and, for the most part, "monotonous." The chromatin pattern is very fine. Nucleoli are not prominent, and nuclear grooves are rarely observed. In general, nuclear pleomorphism is minimal. Despite the fact that foci of bizarre nuclei were reported in more than half of the cases in previous series, they were distributed in a patchy/random manner and comprised < 5% to 10% of overall tumor volume.[7] Tumor cells with hyperchromatic and enlarged nuclei were present in case 1 of our series; however, it only made up < 1% of the whole tumor volume.

Histologic features of MCST such as well-demarcated tumor border, generally bland and monotonous nuclear feature, and low mitotic activity are suggestive of the benign or nonaggressive nature of MCSTs. Clinical behavior of the previous reported MCST cases was favorable.[7] All patients with follow-up information were alive and without evidence of disease. In our series, both tumors were confined in the ovaries at the time of surgery. No distant metastases or peritoneal spread was detected during the follow-up period. However, the number of reported MCSTs is still small, and their follow-up periods are mostly short. Therefore, further studies in larger numbers of cases are necessary to reach definitive conclusions with regard to the behavior and prognosis of MCST.

Immunohistochemical analysis of ovarian MCSTs revealed a characteristic pattern. In addition to diffuse and strong positivity for vimentin and CD10 as reported previously,[7] we found that MCSTs commonly show diffuse nuclear immunoreactivity for β-catenin and WT-1. In general, vimentin and CD10 are of limited use in diagnosing ovarian tumors when each is used as a single marker. Vimentin is positive in various kinds of sex cord-stromal tumors,[16,19,25] endometrioid tumors,[4,6] and mesenchymal tumors.[9,12] CD10 positivity has also been reported in many pure stromal and sex cord-stromal tumors of the ovary.[15] In fact, occasional CD10 positivity was seen in various sex cord-stromal tumors, YSTs, and SOs in our series. However, an ovarian neoplasm that expresses nuclear β-catenin and WT-1, in combination with CD10 and vimentin, is unique. Therefore, we regard this vimentin$^+$/CD10$^+$/WT-1$^+$/β-catenin$^+$ immunophenotype as another key feature that characterizes ovarian

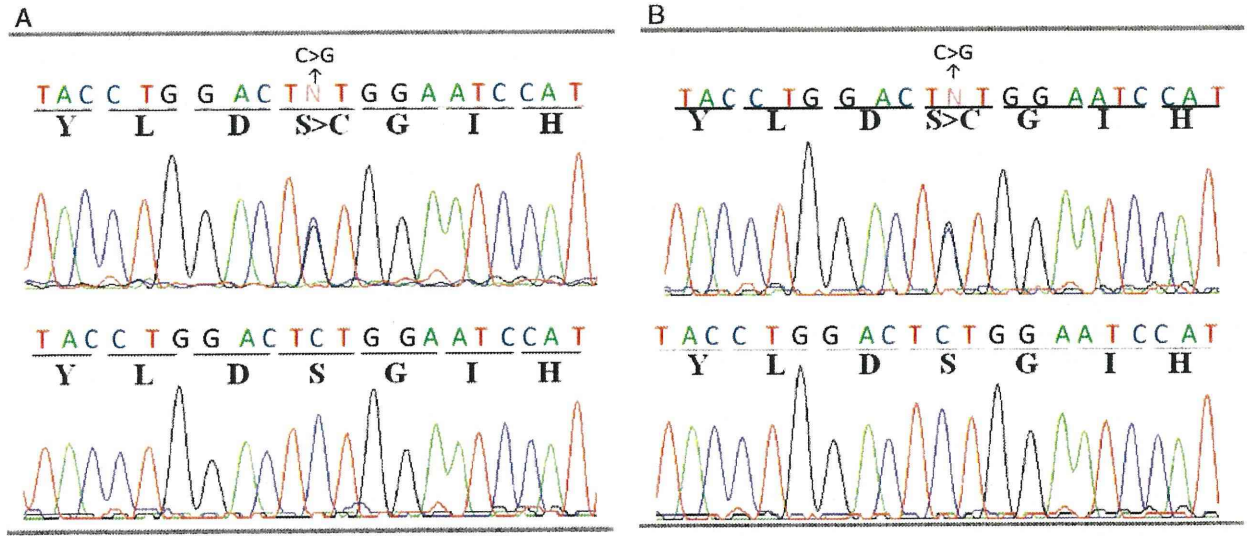

FIGURE 6. In these sequencing chromatograms, the top panel is from MCST, and the bottom panel is the corresponding control sequence. Both cases of ovarian MCST had an oncogenic missense *β-catenin* (*CTNNB1*) mutation, c.98C>G (A: case 1; B: case 2). This mutation causes replacement of serine with cysteine at codon 33, thereby leading to loss of a GSK3β phosphorylation site in the β-catenin protein. C indicates cysteine; D, aspartic acid; G, glycine; H, histidine; I, isoleucine; L, leucine; S, serine; Y, tyrosine.

MCSTs. Consistent with previous reports,[7] the MCSTs in our series were negative for sex cord-stromal markers such as α-inhibin and calretinin. With regard to epithelial markers, focal cytokeratin (Cam 5.2) positivity was reported in 4 of 16 cases in the previous series.[7] In our series, neither of the tumors expressed cytokeratin (Cam 5.2). However, 1 of the cases showed focal positivity for cytokeratin (AE1/AE3).

Much remains unclear regarding the origin of ovarian MCST. Irving and Young[7] suggested a possible stromal origin by excluding other possibilities. We agree that MCST does not fit into the category of surface epithelial stromal tumors or germ cell tumors. Morphologically, these tumors give the impression of stromal or mesenchymal origin, and positive immunoreactivity for vimentin may support the stromal/mesenchymal origin. However, cytokeratin immunoreactivity observed in approximately half of the MCSTs in the previous report and in this study leaves room for a pluripotent nature of the tumor cells. Therefore, on the basis of current evidence, we believe that it is more appropriate to regard MCSTs as "unclassifiable" or as "tumors of uncertain origin" than to classify them as conventional sex cord-stromal tumors.

In this study, we examined β-catenin alterations to understand the pathogenesis of MCSTs. Initially, one of the authors (J.S.) who is a specialist in hepatopancreaticobiliary pathology found morphologic and immunohistochemical similarities between the tumor in case 1 and pancreatic SPN. Monotonous growth of tumor cells with round-to-ovoid, sometimes spindled, nuclei is commonly found in ovarian MCSTs and pancreatic SPNs. Solid areas of ovarian MCST closely resemble those of pancreatic SPN, despite the fact that microcystic changes are usually not present in SPN, and pseudopapillary structures were absent in our MCSTs. Further, diffuse immunoreactivity for CD10 and vimentin is observed both in ovarian MCSTs[7] and pancreatic SPNs.[14] Pancreatic SPN is generally recognized as an epithelial tumor of the pancreas that arises almost exclusively in young women. It is well known for showing aberrant nuclear β-catenin expression that can be detected by immunohistochemistry.[24] In addition, mutations in exon 3 of the *β-catenin* gene are frequently detected in pancreatic SPNs.[1,24] Therefore, we sought to determine whether ovarian MCST shows aberrant nuclear β-catenin expression.

The significance of nuclear β-catenin accumulation in ovarian MCSTs cannot be overemphasized, because it directly suggests that dysregulation of the Wnt/β-catenin pathway is involved in the tumorigenesis. β-catenin-mediated transcription is activated by the Wnt signaling pathway, which plays a crucial role in tumorigenesis. In the absence of Wnt signal, in the normal postembryogenesis period, the levels of β-catenin in cells are controlled by a multiprotein complex that includes adenomatous polyposis coli (APC) and glycogen synthase kinase-3β. Mutations in these components and mutations in *β-catenin* itself lead to excessive accumulation of β-catenin in the nucleus and aberrant stimulation of its target genes, which subsequently results in neoplasia.[17] This abnormal accumulation of β-catenin can be detected immunohistochemically.[13] Therefore, immunohistochemical staining for β-catenin has been used as a surrogate marker for the integrity of canonical Wnt signaling and β-catenin degradation.

In this study, we further performed mutational analyses of exon 3 of the *β-catenin* gene in ovarian MCSTs, because β-catenin-mediated signaling can be constitutively activated by truncation or mutation of serine and threonine residues in exon 3. As a result, we detected the same point mutation, c.98C > G, in exon 3 of *β-catenin* in both tumors. This mutation causes replacement of serine with cysteine at codon 33, leading to the loss of a phosphorylation site in the β-catenin protein. This Ser33 mutation is one of the major oncogenic *β-catenin* mutations that is more commonly detected in benign entities than in malignant tumors.[18] Therefore, we suggest that dysregulation of the Wnt/β-catenin pathway plays an important role in tumorigenesis of ovarian MCSTs. It is not yet clear whether all MCSTs harbor a specific S33C mutation in exon 3 of *β-catenin*. Some other cases may harbor mutations in different regions of this gene. It is also possible that alterations in the *APC* gene or in other genes involved in the Wnt/β-catenin pathway are involved in its tumorigenesis.

A discussion regarding the possible histologic differential diagnoses of ovarian MCSTs is necessary. First, the histology of MCSTs is so unique (ie, dissimilar to any other ovarian tumor) that after encountering a case or being aware of this disease entity there are hardly any other differential diagnoses. However, without knowledge of this entity, ovarian MCST can be confused morphologically with thecoma, AGCT/JGCT, YST, or SO. β-Catenin immunohistochemistry is useful for discriminating MCST from these tumors, because none of these tumors show nuclear β-catenin immunoreactivity. Other ovarian tumors such as sclerosing stromal tumors and steroid cell tumors may also be listed in the differential diagnoses, but not much is known regarding their β-catenin status.

The presence of thick fibrous stroma and growth of monotonous cells are common features observed in ovarian MCSTs and thecomas. However, significant differences are apparent between these 2 entities. Clinically, most thecomas occur in postmenopausal women,[3] and they frequently present with estrogenic symptoms.[23] In contrast, the majority of MCSTs are found in women aged 25 to 45 years. An estrogenic manifestation seems to be extremely rare in reported cases of MCSTs.[7] Macroscopically, thecomas are almost always solid and yellowish. Cystic changes or hemorrhagic changes that are frequently found in MCSTs are rarely observed in thecomas. There are differences in cellular features as well, particularly in the nuclear morphology. Cells with polygonal or spindle-shaped nuclei are far more prominent in thecomas than in MCSTs. Immunohistochemically, α-inhibin and calretinin, which are positive in most thecomas,[26] are negative in MCSTs. A variant of

thecoma, luteinized thecoma, often shows a microcystic growth pattern and may mimic MCST. However, luteinized thecomas are almost always bilateral and usually associated with sclerosing peritonitis. Immunohistochemically, luteinized thecomas do not show nuclear β-catenin accumulation. Luteinized cells in luteinized thecomas are positive for α-inhibin and calretinin.[22] Therefore, these markers should be useful for distinguishing an ovarian MCST from a luteinized thecoma.

There are certain similarities between MCSTs and AGCTs. AGCTs frequently exhibit a solid-cystic gross appearance, and hemorrhagic changes are occasionally seen. Monotonous growth of tumor cells is also common in MCSTs and AGCTs. However, significant differences are apparent in the histology between MCSTs and AGSTs. Tumor cells of MCSTs are predominantly round and lack nuclear grooves. In contrast, AGCT cells are short spindled, and they have characteristic nuclear grooves. In addition, microcystic/macrocystic structures of MCSTs differ from microfollicular/macrofollicular structures of AGCTs. In MCSTs, the tumor cells do not line up toward the cystic lumen. Structures such as Call-Exner bodies are absent in MCSTs. Recent studies have shown that a somatic mutation in the *FOXL2* gene (c.402C > G) is present in almost all (86 of 89, 97%) morphologically defined AGCTs.[2,8,10,20,21] In this study, we demonstrated the absence of this mutation in ovarian MCSTs. Hence, we expect that ovarian AGCTs and MCSTs also differ significantly in their genetic background. JGSTs tend to have cells with larger and more pleomorphic nuclei compared with MCSTs. Furthermore, mitotic figures are much more frequently found in JGSTs (median, 9.8/10 high-power fields).[19] In problematic cases, immunohistochemistry for α-inhibin and calretinin should be applied, because most AGCTs and JGCTs are positive for these markers.[19,26] Distinguishing an MCST from a sclerosing stromal tumor should not be too difficult, as microcysts are not a feature of sclerosing stromal tumors. Steroid cell tumors frequently have a hormonal presentation, and they typically show diffuse proliferation of tumor cells with an inconspicuous stroma. An intervening thick fibrous stroma, which is commonly seen in MCSTs, is usually absent in ovarian steroid cell tumors. As rare Sertoli-Leydig cell tumors have microcysts somewhat similar to those of MCSTs, thorough sampling of the tumor is recommended. Well-sampled Sertoli-Leydig cell tumors almost always reveal foci of typical Sertloi cell and Leydig cell growth. At low magnification, MCSTs can resemble YSTs, because both tumors show microcystic and/or reticular structures and frequent hemorrhagic changes. However, MCSTs do not show strong nuclear atypia that can be seen in YSTs. Immunohistochemistry for α-fetoprotein or SALL4 can help to distinguish between these tumors, because these markers are expressed by YSTs but not by MCSTs. SOs have a broad range of histology, and some may mimic MCSTs. In our experience, typical colloid that fills the follicles of SO is not observed in the cystic lumen of MCSTs. In difficult cases, we recommend performing immunohistochemistry for thyroid transcription factor-1, a known marker for thyroid tumors not expressed in MCSTs.

Finally, we mention ovarian SPN as a potential differential diagnosis for MCSTs. Deshpande et al[5] recently reported 3 cases of ovarian tumors that revealed similar morphologic and immunohistochemical features to pancreatic SPN and proposed the entity "solid pseudopapillary tumor of the ovary." In our observations, morphologic features of MCST and SPN were similar in some aspects. Growth of round-to-spindled monotonous cells was common in both tumors, and solid areas of growth in MCSTs and SPNs closely resembled each other. However, certain differences were also apparent. Pseudopapillary structure, which is characteristic of SPNs, was absent in MCSTs. Immunoreactivity for markers such as WT-1, CD56, and progesterone receptor also differed between SPNs and MCSTs. Interestingly, in the report by Deshpande et al,[5] β-catenin nuclear immunoreactivity was observed in all 3 ovarian SPN cases. Although a mutation analysis was not performed in their study, dysregulation of Wnt/β-catenin signaling could theoretically be involved in the development of ovarian SPNs. Their results and our results suggest a possible link between ovarian SPNs and MCSTs. We hope to further examine similarities and differences between ovarian MCSTs and SPNs in the future on the basis of a larger number of cases.

In conclusion, we presented the distinct features of ovarian MCST from morphologic, immunohistochemical, and genetic viewpoints. Dysregulation of Wnt/β-catenin signaling is involved in the pathogenesis of ovarian MCST. The findings presented here provide insight into this unique entity and will facilitate future studies.

ACKNOWLEDGMENT

The authors thank Yumiko Nagano for her tremendous technical support.

REFERENCES

1. Abraham SC, Klimstra DS, Wilentz RE, et al. Solid-pseudopapillary tumors of the pancreas are genetically distinct from pancreatic ductal adenocarcinomas and almost always harbor beta-catenin mutations. *Am J Pathol.* 2002;160:1361–1369.
2. Benayoun BA, Caburet S, Dipietromaria A, et al. Functional exploration of the adult ovarian granulosa cell tumor-associated somatic FOXL2 mutation p.Cys134Trp (c.402C > G). *PLoS One.* 2010;5:e8789.
3. Björkholm E, Silfverswärd C. Theca-cell tumors: clinical features and prognosis. *Acta Radiol Oncol.* 1980;19:241–244.
4. Dabbs DJ, Sturtz K, Zaino RJ. The immunohistochemical discrimination of endometrioid adenocarcinomas. *Hum Pathol.* 1996;27:172–177.
5. Deshpande V, Oliva E, Young RH. Solid pseudopapillary neoplasm of the ovary: a report of 3 primary ovarian tumors resembling those of the pancreas. *Am J Surg Pathol.* 2010;34:1514–1520.
6. Eichhorn JH, Young RH, Clement PB. Sertoliform endometrial adenocarcinoma: a study of four cases. *Int J Gynecol Pathol.* 1996;15:119–126.
7. Irving JA, Young RH. Microcystic stromal tumor of the ovary: report of 16 cases of a hitherto uncharacterized distinctive ovarian neoplasm. *Am J Surg Pathol.* 2009;33:367–375.